artery is unclear. The platelet aggregation test using light transmission aggregometry (LTA) is currently the gold standard method of evaluating platelet function. Although this test is useful for detecting platelet function deficiencies, it is not adequate for estimating high platelet reactivity, has poor reproducibility, requires skillful manipulation, and is time consuming [15–17].

A new flow-chamber system was recently developed to quantitatively evaluate the growth of PTF using whole blood samples under flow conditions [18,19]. This device, the Total Thrombus-formation Analysis System (T-TAS, Fujimori Kogyo Co., Yokohama, Kanagawa), analyzes the process of PTF by monitoring the continuous pressure increase in the capillary channels of two types of microchips with thrombogenic surfaces. The first chip, the PL chip, contains 25 capillary channels coated with collagen. A whole blood sample anticoagulated with the thrombin inhibitor hirudin is applied to the chip under constant flow speed until occlusion. The continuous increase in the inner pressure is measured, reflecting the specific thrombogenicity mainly mediated by platelets. The second chip, the AR chip, contains a single capillary channel coated with collagen and tissue thromboplastin. Collected citrated whole blood is recalcified immediately before testing, and then tested in a similar way, allowing for the assessment of parameters related to the formation of a platelet thrombus rich in fibrin fibers, representing whole blood thrombogenicity under flow conditions [18]. This system is reported to be useful for evaluating the effects of some clinical anticoagulants (e.g., heparin, argatroban, abciximab, aspirin, $P2Y_{12}$ antagonist) [18,19], human blood products (prothrombin complex concentrates, fresh frozen plasma) [20], and factor VIII or IXa deficiency [21].

In the present study, we aimed to characterize the effectiveness of this system for evaluating the thrombogenicity of whole blood under flow conditions in healthy individuals by comparing the measurements with those of other standard platelet function tests. In addition, we investigated some blood constituents that could affect the measurements obtained using this system.

## Materials and Methods

### *Subjects*

Healthy volunteers (11 men, 20 women), between 25 and 62 (mean ± SD, 39 ± 11) years of age, were recruited from Keio University School of Medicine. Individuals taking medication or dietary supplements within the previous 2 weeks that could affect platelet function or coagulation were excluded. All individuals were apparently healthy based on a medical questionnaire. Among them, 26 subjects received regular physical checkups within 6 months in the facility, and the following data were recorded. Mean ± SD body mass index (21 ±2.7 kg/m$^2$), blood pressure (117 ± 17/69 ± 11 mmHg), glucose (96 ± 9 mg/dl), triglyceride (79 ± 40 mg/dl), HDL-cholesterol (67 ± 18 mg/dl), and LDL-cholesterol (110 ± 31 mg/dl). The study was conducted according to the guidelines of the Declaration of Helsinki, and all procedures involving human subjects were approved by the Ethics Committee of Keio University. Written informed consent was obtained from all subjects before beginning the study.

### *Blood Samples*

Blood samples were collected from the antecubital vein with a 21-gauge butterfly needle into the following tubes: a Hirudin Blood Tube (MP0600: Dynabyte GmbH, Munich, Germany, final concentration of hirudin: 25 μg/ml), a vacuette tube (31–114: Nipro neotube, Nipro, Japan) and blood collection tubes (VP-CW050K, VP-C050K, VP-P052K: Venoject II, Terumo, Japan). Plasma or serum samples to measure biomarkers were prepared by centrifuging whole blood at 2500 rpm for 10 min at room temperature. All platelet function tests were performed from 1 to 4 hours after blood sample collection.

### *Microchip Flow-chamber System*

The PTF process was monitored quantitatively using the T-TAS as previously reported [18,19]. Briefly, this system analyzes PTF generation by monitoring the continuous pressure increase in the capillary channels of each of two microchips with thrombogenic surfaces.

One chip, the PL chip, contains 25 capillary channels 40 μm wide × 40 μm deep coated with type I collagen [19]. A whole blood sample (320 μl) anticoagulated with the thrombin inhibitor hirudin is applied to the chip under constant flow until occlusion. The continuous increase in the inner pressure is measured, reflecting the specific thrombogenicity mainly mediated by platelets in the absence of coagulation and fibrinolysis pathways [19,22]. Another chip, the AR chip, contains a single capillary channel 300 μm wide × 120 μm deep coated with type I collagen plus tissue thromboplastin [18]. Whole blood taken with 3.13% sodium citrate is mixed with $CaCl_2$ and corn trypsin inhibitor (CTI) immediately before testing to restore the coagulation system except for Factor XII, and the mixture of 450 μl is tested similarly under constant shear rate (300 $s^{-1}$), allowing for the measurement of parameters related to the formation of the fibrin-rich platelet thrombus, representing whole blood thrombogenicity under flow. Activity of the tissue thromboplastin coated on the AR chip and the effect of CTI on intrinsic coagulation pathway were assessed elsewhere (Figs. S1 and S2).

The typical flow pressure patterns and measured parameters using the PL or AR chips are depicted in Fig. 1. The PTF starting time was defined as $T_{10}$ (min: s), the time in minutes for pressure to reach 10 kPa from baseline. Based on the pressure increase, the time required to reach 60 kPa, $T_{60}$, was defined as the occlusion time for the PL chip [22], and similarly, the time required to reach 80 kPa ($T_{80}$) was defined as the occlusion time for the AR chip. The growth rates of PTF were calculated as $T_{60}$ minus $T_{10}$ ($T_{10\text{-}60}$) or $T_{80}$ minus $T_{10}$ ($T_{10\text{-}80}$). AUC refers to the area under the flow pressure curve; $AUC_{10}$, until 10 min for the PL chip, and $AUC_{30}$, until 30 min for the AR chip. All of the measurements were performed under a constant flow speed of 12, 18, and 24 μl/min, corresponding to shear rates of 1000, 1500, and 2000 $s^{-1}$ for the PL chip, and 10 μl/min, corresponding to 300 $s^{-1}$ for the AR chip.

### *Platelet Aggregometry*

The light transmission aggregometry (LTA) test was performed using 3.8% citrated whole blood samples. Platelet-rich plasma was prepared by centrifuging at 700 rpm for 15 min and platelet-poor plasma was prepared by centrifuging at 2500 rpm for 10 min at room temperature. Platelet-rich plasma was adjusted to 300,000 platelet counts/μl using platelet-poor plasma. Thereafter, 22 μl of each agonist was added to 200 μl of the adjusted platelet-rich plasma. Platelet aggregation was induced by a final concentration of 5 μmol/l adenosine diphosphate (ADP; Trinity Biotech, Co., Wicklow, Ireland), 2 μg/ml collagen (Takeda Pharmaceutical International GmbH, Zurich, Switzerland), 10 μmol/l epinephrine (Daiichi Sankyo Co., Ltd., Tokyo, Japan) or 1.2 mg/ml ristocetin (Nacalai Tesque, Kyoto, Japan). The rate of maximum platelet aggregation (MPA) and area under the aggregation curve (AUC) were measured using Easy Tracer ET-800 (Tokyo Koden, Tokyo, Japan).

### *VerifyNow P2Y12 Assay*

The VerifyNow P2Y12 system (Accumetrics, San Diego, CA) is a whole-blood, light transmission-based optical detection assay that measures ADP-induced platelet aggregation in a cartridge containing fibrinogen-coated beads. The blood sample in a 3.13% sodium citrate tube was applied to the cartridge with two channels according to the manufacture's instruction; one contained 20 μmol/l of ADP and

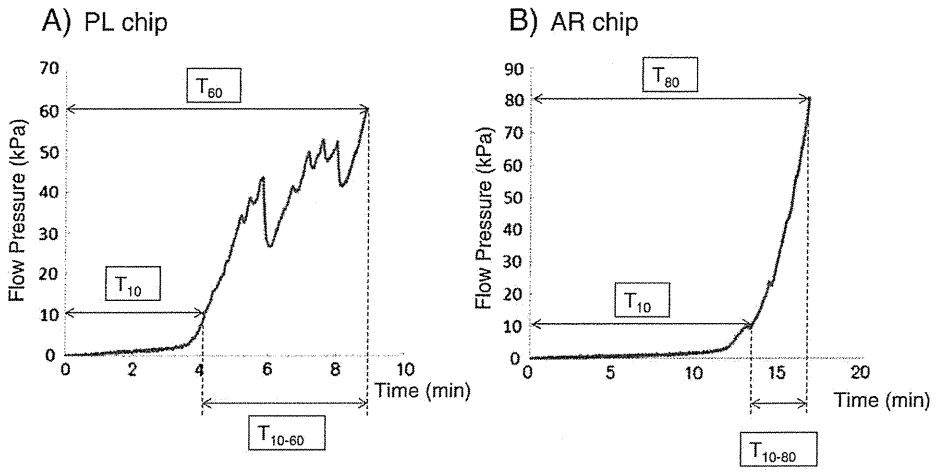


**Fig. 1.** T-TAS flow pressure curves and parameters. A) PL chip. $T_{10}$: time from baseline pressure to reach 10 kPa (PTF starting time). $T_{60}$: time to reach 60 kPa (occlusion time). $T_{10\text{-}60}$: $T_{60}$ minus $T_{10}$ (PTF growth rates). $AUC_{10}$: area under the flow pressure curve for 10 min. B) AR chip. $T_{10}$: time from baseline pressure to reach 10 kPa. $T_{80}$: time to reach 80 kPa. $T_{10\text{-}80}$: $T_{80}$ minus $T_{10}$. $AUC_{30}$: area under the flow pressure curve for 30 min.

22 nmol/l of prostaglandin $E_1$, the other contained iso-thrombin receptor agonist peptide. The results are expressed as P2Y12 reaction units (PRU).

*Platelet Function Analyzer-100*

The platelet function analyzer (PFA)-100 (Dade-Behring, Marburg, Germany) is a device used to assess platelet function under high-shear rates (5000–6000 $s^{-1}$) using citrated whole blood. We used 3.8% sodium citrate in this study [23,24]. The sample is subjected to constant flow through a capillary to a microscopic aperture cut into the membrane coated with collagen and epinephrine (C/EPI) or collagen and ADP (C/ADP). These agonists and high-shear rates induce platelet attachment, activation, and aggregation, resulting in occlusion of the aperture. The time required for full occlusion is reported as the closure time (CT). In this study, CT values greater than 300 s were regarded as 300 s for statistical analysis.

*Complete Blood Count Tests and Biomarkers*

Complete blood count tests were performed using the Sysmex KX-21, an automated hematology analyzer (Sysmex Corporation, Kobe, Japan). Plasma levels of biomarkers were measured using commercially available kits as follows; VWF:CB (VWF-CBA enzyme-linked immunosorbent assay [ELISA]; PROGEN Biotechnik GmbH, Germany), VWF:Ag (IMUBIND® VWF Activity ELISA; American Diagnostica, Stamford, CT), ADAMTS13:Ag (IMUBIND® ADAMTS13 ELISA; American Diagnostica), ADAMTS13:Ac (FRETS-VWF73, Peptide Institute, Inc., Osaka, Japan), Fibrinogen:Ag (Human Fibrinogen ELISA Kit; Innovative Research, Novi, MI), plasminogen activator inhibitor (PAI)-1:Ag (IMUBIND Plasma PAI-1 ELISA; American Diagnostica), PAI-1:Ac (PAI-1, Active, Human, ELISA kit; Innovative Research), glycocalicin (Glycocalicin EIA Kit; Takara Bio Inc, Shiga, Japan), high sensitive C-reactive protein (hs-CRP; CircuLex High-Sensitivity CRP ELISA Kit; CycLex Co., Ltd., Nagano, Japan).

*Statistical Analysis*

Data are shown as the mean ± SD unless indicated otherwise. The Shapiro-Wilk test was performed to assess for the normal distribution of all measured parameters. Correlations of parametric or non-parametric data were analyzed with Pearson's correlation coefficient or Spearman's correlation coefficient, respectively. Statistical analysis was performed using SPSS version 16.0 (SPSS Inc, Chicago, IL). Two-tailed values were reported, and P values of less than 0.05 were considered statistically significant. The reference intervals of the measurements were defined as the range within 95% confidence intervals. Figures were prepared using Graph Pad Prism (Graph Pad Software Inc., San Diego, CA).

## Results

*Measurements by T-TAS*

The individual time-dependent continuous inner pressure increase in the microchips was represented as a waveform (Fig. 2). The starting and ending points of PTF using the PL or AR chip varied among healthy subjects, possibly characterizing the individual potential for thrombus formation under blood flow conditions.

The results (mean ± SD, range) of the PTF starting time ($T_{10}$), occlusion time ($T_{60}$ or $T_{80}$), growth rates ($T_{10\text{-}60}$ or $T_{10\text{-}80}$), and AUC ($AUC_{10}$ or $AUC_{30}$) using the PL or AR chip are summarized in Table 1. Intra-assay coefficients of variation (CV) in PL chip measurements (1500 $s^{-1}$) were as follows: $T_{10}$ 6.0%, $T_{60}$ 4.2%, $T_{10\text{-}60}$ 6.2%, $AUC_{10}$ 2.5% (n = 5), and in AR chip measurements: $T_{10}$ 7.9%, $T_{80}$ 6.0%, $T_{10\text{-}80}$ 20.2%, $AUC_{30}$ 5.0% (n = 4). In the PL chip, $T_{10}$ and $T_{60}$ both decreased in accordance with an increase in shear rates. Furthermore, $T_{10\text{-}60}$ was also decreased, indicating that the shear rates accelerated the growth rate of PTF. Consequently, a shear-dependent increase in $AUC_{10}$ was observed, indicating a comprehensive parameter related to the platelet-mediated thrombogenicity under high shear stress. In addition, the standard deviation (SD) of $T_{10}$ at 1000 $s^{-1}$ was greater than at 1500/2000 $s^{-1}$, and SD of $T_{10\text{-}60}$ at 1000/1500 $s^{-1}$ was greater than that at 2000 $s^{-1}$, whereas the SD of $T_{60}$ and $AUC_{10}$ was almost the same. Accordingly, the difference in individual thrombogenicity might be well expressed by the $T_{10}$ and $T_{10\text{-}60}$ at low shear rates. The distribution of measurements illustrates the characteristics of these parameters (Fig. 3).

In this study, the reference intervals of the measurements were defined as the range within 95% confidence intervals. Among the 31 subjects, a 55-year-old woman showed decreased $T_{10}$ in the PL chip at 2000$s^{-1}$ (1:01), possibly related to enhanced thrombogenicity, although she exhibited no abnormalities in the LTA, VerifyNow P2Y12 assay, and PFA-100. Among the 31 subjects, 8 showed prolonged $T_{10}$, $T_{10\text{-}60}$, or $T_{60}$, or reduced $AUC_{10}$, possibly related to reduced thrombogenicity. Of

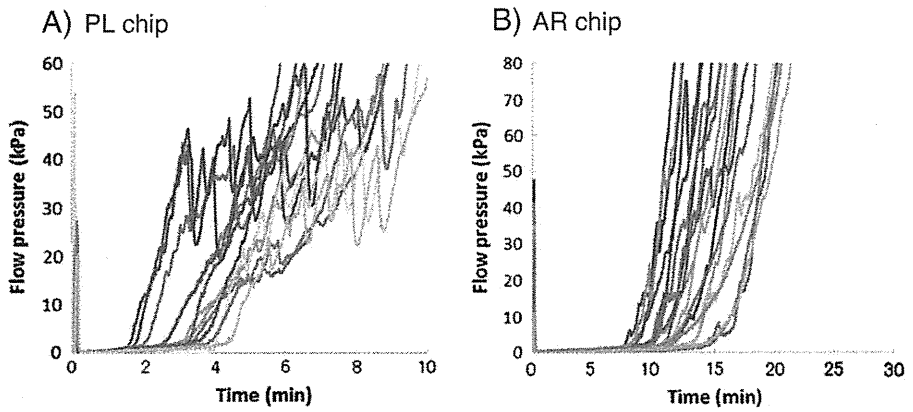


**Fig. 2.** Variations in individual time-dependent flow pressure curves depicted as superimposed waveforms. A) Measurements by PL chip from 13 subjects. B) Measurements by AR chip from 19 subjects.

these 8, 3 exhibited abnormalities in other tests. A 31-year-old woman showed prolonged $T_{10}$ in the PL at 1000 $s^{-1}$ (5:53) and in the AR (16:20) with reduced ristocetin-induced MPA (49.0%) and prolonged C/ADP (185 s). A 52-year-old man exhibited a prolonged $T_{60}$ (6:28) with reduced epinephrine-induced MPA (35.7%) and reduced PRU (175). A 28-year-old man showed only reduced $AUC_{10}$ in the PL chip at 2000$s^{-1}$ (262.7), although he had reduced epinephrine-induced MPA (26.7%) and AUC (6679.9), ADP-induced MPA (53.6%) and AUC (13979.6), collagen-induced MPA (49.2%) and AUC (7444.9), and prolonged C/EPI (>300 s). The remaining 5 subjects exhibited no abnormalities in other tests.

*Other Platelet Function Tests*

Platelet function tests of the healthy subjects were performed using the LTA, VerifyNow P2Y12 assay, and PFA-100 (Fig. 4), and the results were compared with the T-TAS measurements. In LTA, 4 of 31 subjects showed abnormalities; 3 of these 4 had abnormalities in T-TAS. Among the remaining subjects, a 57 year-old man exhibited reduced ADP-induced MPA (55.4%) with prolonged C/ADP (155 s), but no abnormalities in the T-TAS. In the VerifyNow P2Y12 assay, only one subject showed reduced PRU (175) with normal T-TAS measurements. In the PFA-100, two subjects showed prolonged C/EPI (>300). Of these, one showed reduced epinephrine-induced MPA (26.7%) with slight abnormality in the T-TAS (reduced $AUC_{10}$ at 2000 $s^{-1}$), and the other showed normal epinephrine-induced MPA (83.4%) with no abnormality in the T-TAS. And two subjects showed prolonged C/ADP. Of these, one exhibited prolonged $T_{10}$ in the PL at 1000 $s^{-1}$ and the other had no abnormality in the T-TAS.

*Correlation between T-TAS and other Platelet Function Tests*

In the PL chip, $T_{10}$ was correlated with C/EPI and C/ADP (Fig. 5), and $AUC_{10}$ was correlated with C/EPI (data not shown) under all of the shear rate conditions. Furthermore, the relationship was enhanced in accordance with an increase in the shear rates. Thus, the findings from the PL chip were associated with those of the PFA-100 in many respects, indicating that its characteristics were related to high shear-induced PTF. In addition, $T_{60}$ and $AUC_{10}$ correlated with the AUC of collagen-induced platelet aggregation curve under all shear rate conditions ($|r| = 0.404 \sim 0.531$). In the AR chip, $T_{10\text{-}80}$, reflecting the rate of PTF, was significantly correlated with C/ADP ($r = -0.366$, $p = 0.043$), although few AR measurements were associated with other platelet function tests. The VerifyNow P2Y12 assay values were not significantly associated with the parameters of the T-TAS.

*T-TAS and CBC/biomarkers*

To identify the blood constituents that would affect this system, we investigated the correlations between CBC, hematocrit, VWF, fibrinogen, ADAMTS13, PAI-1, hs-CRP, and glycocalicin. The results of CBC, VWF, and fibrinogen tests are shown in Table 2. Interestingly, platelet counts were correlated with all parameters in the AR chip (Fig. 6), and mostly with those in the PL chip. The VWF results were not associated with any of the T-TAS measurements. Fibrinogen was associated with $T_{10}$ in the PL at 1000 $s^{-1}$. Other biomarkers tested were irrelevant. For reference, as previously reported [38], C/EPI and C/ADP of the PFA-100 were correlated with VWF ($r = -0.501, -0.382$). The VerifyNow P2Y12 assay values were associated with red blood cells, hemoglobin, and hematocrit ($r = -0.725, -0.788, -0.732$, respectively).

**Table 1**
Mean ± SD, range of T-TAS measurements (min:s or min · kPa).

| | PL chip | | | AR chip | |
|---|---|---|---|---|---|
| | 1000 $s^{-1}$ | 1500 $s^{-1}$ | 2000 $s^{-1}$ | 300 $s^{-1}$ | |
| $T_{10}$ | 3:44 ± 1:02 (1:57–6:01) | 2:43 ± 0:51 (1:10–4:30) | 2:32 ± 0:41 (1:00–3:50) | $T_{10}$ | 11:39 ± 2:15 (8:39–16:44) |
| $T_{60}$ | 8:00 ± 1:14 (5:51–10:10) | 5:47 ± 1:36 (3:03–9:26) | 4:55 ± 1:12 (3:13–7:57) | $T_{80}$ | 15:48 ± 2:56 (11:42–21:21) |
| $T_{10-60}$ | 4:16 ± 1:04 (2:16–6:30) | 3:03 ± 1:03 (1:26–5:07) | 2:23 ± 0:48 (1:05–4:35) | $T_{10-80}$ | 4:08 ± 1:11 (2:12–6:42) |
| $AUC_{10}$ | 271.1 ± 58.2 (176.6–369.1) | 369.1 ± 71.8 (196.0–487.4) | 396.6 ± 55.8 (262.7–492.5) | $AUC_{30}$ | 1318.5 ± 203.2 (924.9–1576.1) |

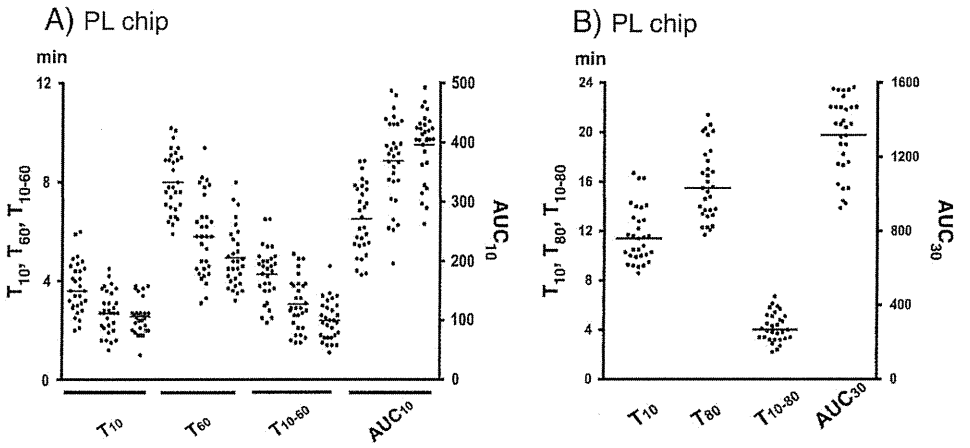


**Fig. 3.** Distribution of the T-TAS measurements from 31 healthy subjects. A) PL chip. In each measurement, shear rates were 1000, 1500, and 2000 $s^{-1}$ from left, middle, and right, respectively. B) AR chip. Shear rate: 300 $s^{-1}$. $T_{10}$: PTF starting time. $T_{60}$, $T_{80}$: occlusion time. $T_{10\text{-}60}$, $T_{10\text{-}80}$: PTF growth rates. $AUC_{10}$, $AUC_{30}$: area under the flow pressure curve until 10 or 30 min.

## Discussion

The process of thrombus formation is a complex pathway in which blood constituents, vessel wall function, and blood flow are integrated (Virchow's triad) [25,26]. Many blood tests have been developed to assess factors related to hemorrhagic or thrombotic diathesis, such as platelets, coagulation, fibrinolysis, and endothelial cell function, although it remains unclear which clinical test is most appropriate for evaluating total thrombogenicity.

The T-TAS, a flow chamber system, uses whole blood samples, and flow on thrombogenic surfaces (collagen: PL chip; collagen plus thromboplastin: AR chip) is measured under various shear rate conditions. Accordingly, this system allows for measurements of at least two factors of the triad, blood constituents and flow, and the blood volume required is practical for clinical application. The starting and ending points of occlusion by clotting are monitored as the pressure is increased (Fig. 1), allowing for measurement of the parameters possibly linked to individual thrombogenicity. The pressure increase is represented as a waveform specific to each individual (Fig. 2). The distribution of the occlusion starting time ($T_{10}$), ending time ($T_{60}$ or $T_{80}$), growth rate ($T_{10\text{-}60}$ or $T_{10\text{-}80}$), and AUC ($AUC_{10}$ or $AUC_{30}$) varied among healthy subjects (Fig. 3). These findings suggested that the measurement

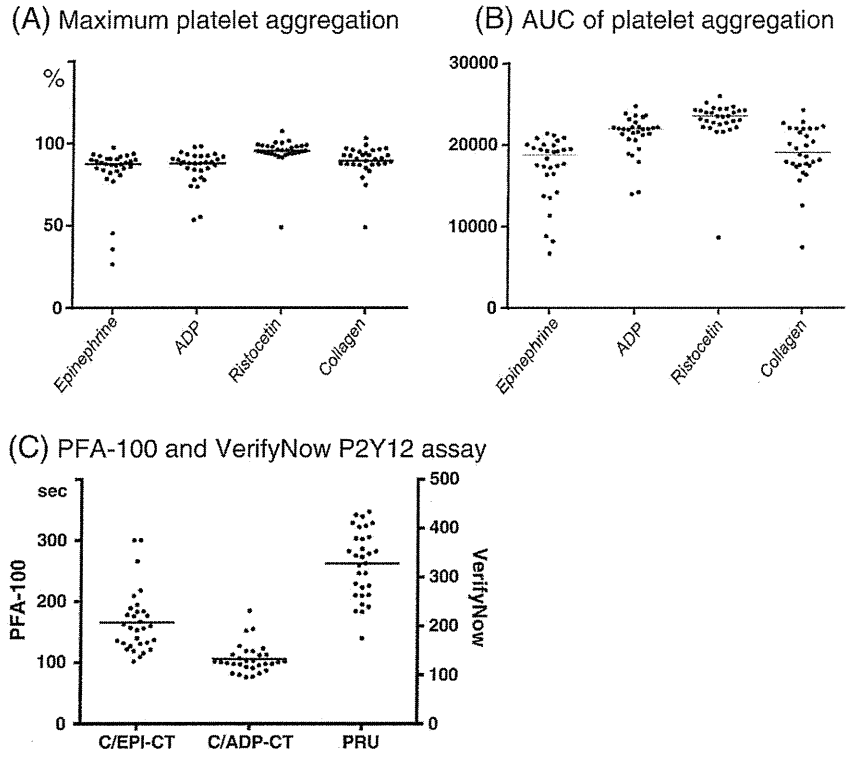


**Fig. 4.** Distribution of measurements by platelet function tests from 31 healthy subjects. A) LTA maximum platelet aggregation by agonists. B) AUC (area under curve) of platelet aggregation curve induced by agonists. C) Closure time of the C/EPI and C/ADP cartridge by PFA-100 (left), and PRU of the P2Y12 assay by VerifyNow (right).

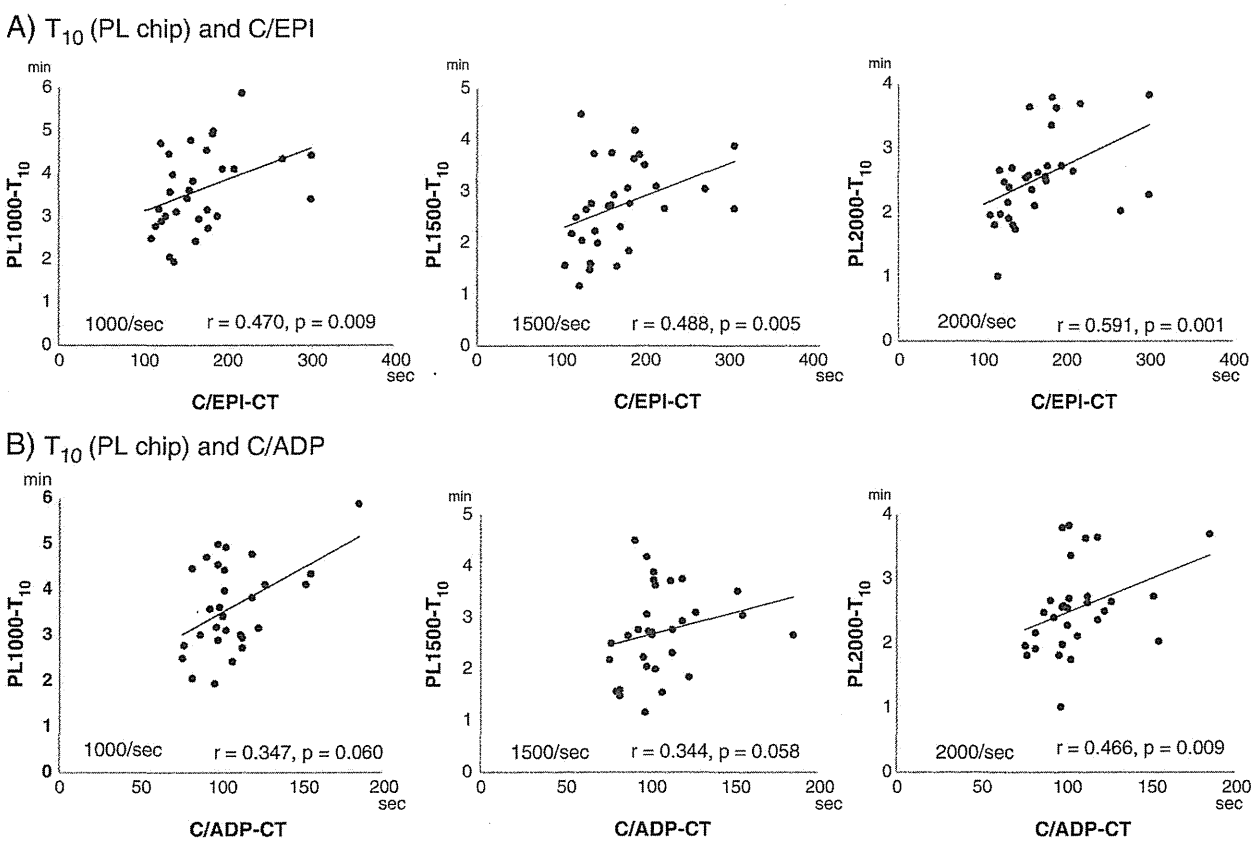


**Fig. 5.** Correlation of PTF starting time ($T_{10}$) by T-TAS/PL-chip and the closure time of C/EPI (top) and C/ADP (bottom) by PFA-100. Shear rates were 1000, 1500, and 2000 $s^{-1}$ from left, middle, and right, respectively. r, correlation coefficient. p, probability value.

parameters of the T-TAS reflect individual characteristics of thrombus formation.

In the PL chip, the thrombus is formed under high shear rates without the generation of thrombin, thus the measurements reflect the parameters mainly mediated by platelets in the absence of coagulation and fibrinolysis pathways. At high-shear rates, the interaction between the platelet membrane glycoprotein GPIb-IX-V complex and collagen-bound VWF plays a key role in the first step of platelet adhesion [27,28]. As the shear rates increased, $T_{10}$, $T_{60}$, $T_{10\text{-}60}$ were decreased and $AUC_{10}$ was increased (Table 1, Fig. 3), supporting the involvement of the GPIb-IX-V/VWF interaction in these measurements. Previous reports showed contribution of the interaction during the thrombus formation in the T-TAS using GPIb inhibitor [19] and anti-VWF monoclonal antibodies [32].

The standard deviation of $T_{10}$, $T_{60}$, and $T_{10\text{-}60}$ in the PL chip diminished in accordance with an increase in the shear rate, thus individual differences might be poorly expressed under higher shear rate conditions. It is noteworthy that $T_{10}$ and $AUC_{10}$ showed a shear-dependent correlation with C/EPI or C/ADP. Because the PFA-100 uses citrated whole blood under high-shear rates (5000–6000 $s^{-1}$), it is reasonable that the results of the PL chip were associated with the results of the PFA-100 in many respects, based on its characteristics related to high shear-induced PTF [29]. We speculate that the PL chip might detect individual differences more sensitively than the PFA-100, because of the lower shear rates and the use of only collagen as a physiologic agonist. In contrast, however, the results of the LTA and VerifyNow P2Y12 assay rarely correlated with those of the PL chip. In the LTA, only the AUC of the collagen-induced platelet aggregation curve correlated with $T_{60}$ and $AUC_{10}$ under all shear rate conditions ($|r| = 0.404 \sim 0.531$). For stable platelet adhesion on the collagen in subendothelium after GPIb-IX-V/VWF interaction, subsequent activation of integrin GPIIb-IIIa and collagen receptors is involved in the binding to fibrinogen, VWF, and collagen [1,2]. The collagen-induced AUC might be associated with the platelet reactivity to collagen under flow conditions in a certain way in the PL chip. Interestingly, fibrinogen levels were associated with a measurement in the PL chip (Table 2), suggesting the contribution of fibrinogen as a bridging factor among platelets, and some clinical reports identified the fibrinogen level as a possible risk factor for cardiovascular disease [30,31]. It is not clear why VWF levels were not associated with any of T-TAS measurements (Table 2). Patients with VWD were reported to exhibit delayed thrombus formation in the T-TAS measurements [32,33]. In healthy subjects, however, thrombus formation should be the consequence of comprehensive reactions in addition to the GPIb-IX-V/VWF interaction, thus the VWF levels alone were not supposed to correlate with the T-TAS measurements. Within normal range of VWF level, higher shear rates might be necessary to detect the effect of VWF levels on PTF in this system. Consequently, the parameters measured in the PL chip are thought to reflect platelet reactivity to adhesion on the collagen surface under whole blood flow conditions with high shear rates between 1000 and 2000$s^{-1}$.

In the AR chip, citrated whole blood was recalcified and subjected to flow on the surface coated with collagen and tissue thromboplastin under shear rates of 300 $s^{-1}$, corresponding to those in large-sized arteries [34]. Thus, the extrinsic coagulation pathway and platelet adhesion/activation on the collagen surface under flow were totally involved in the process of fibrin-rich PTF in this microchip. The starting and ending points of individual waveforms clearly varied among healthy subjects, although the rates of thrombus formation

**Table 2**
Correlation of T-TAS measurements with blood constituents.

| | WBC | HCT | PLT | VWF:CB | VWF:Ag | Fibrinogen |
|---|---|---|---|---|---|---|
| **PL-1000** | | | | | | |
| $T_{10}$ | −0.219 | −0.035 | −0.304 | −0.101 | −0.201 | 0.375 |
| $T_{60}$ | −0.060 | 0.373 | −0.398 | −0.026 | −0.077 | 0.24 |
| $T_{10\text{-}60}$ | 0.143 | 0.503 | −0.162 | 0.069 | 0.096 | -0.087 |
| $AUC_{10}$ | 0.189 | −0.128 | 0.412 | 0.090 | 0.195 | -0.315 |
| **PL-1500** | | | | | | |
| $T_{10}$ | 0.021 | −0.010 | −0.359 | −0.203 | −0.221 | 0.137 |
| $T_{60}$ | −0.223 | 0.213 | −0.502 | −0.016 | −0.023 | 0.146 |
| $T_{10\text{-}60}$ | −0.355 | 0.336 | −0.471 | 0.140 | 0.103 | 0.111 |
| $AUC_{10}$ | 0.150 | −0.138 | 0.484 | 0.090 | 0.086 | −0.146 |
| **PL-2000** | | | | | | |
| $T_{10}$ | 0.079 | 0.083 | −0.164 | −0.201 | −0.181 | 0.197 |
| $T_{60}$ | −0.223 | 0.193 | −0.355 | −0.093 | −0.037 | 0.203 |
| $T_{10\text{-}60}$ | −0.403 | 0.152 | −0.395 | 0.031 | −0.012 | 0.138 |
| $AUC_{10}$ | 0.095 | −0.145 | 0.305 | 0.115 | 0.024 | −0.266 |
| **AR** | | | | | | |
| $T_{10}$ | −0.103 | 0.136 | −0.411 | −0.019 | −0.164 | 0.135 |
| $T_{80}$ | −0.091 | 0.193 | −0.520 | −0.004 | −0.095 | 0.025 |
| $T_{10\text{-}80}$ | −0.030 | 0.245 | −0.503 | 0.026 | 0.041 | −0.179 |
| $AUC_{30}$ | 0.115 | −0.169 | 0.509 | 0.009 | 0.087 | −0.047 |

Values shown are correlation coefficients. Enclosed figures are statistically significant ($p < 0.05$). WBC: white blood cell counts. HCT: hematocrit. PLT: platelet counts. VWF CB: von Willebrand factor collagen binding activity. VWF Ag: von Willebrand factor antigen. Mean ± SD (range) of each measurement was as follows: WBC ($x10^2/\mu l$), 50 ± 12 (24–78); HCT (%), 36.9 ± 3.3 (30.6–44.6); PLT ($x10^3/\mu l$), 224 ± 44 (155–342); VWF:CB (%), 95.2 ± 22.2 (54.3–142.9); VWF:Ag (%), 112.8 ± 39.9 (48.3–210.5); Fibrinogen (mg/dl), 275.9 ± 55.9 (157.8–402.2).

seemed almost constant (Fig. 1B). Accordingly, $T_{10}$ or $T_{80}$ could be a useful parameter for evaluating individual differences. Unlike the PL chip, $T_{10}$, $T_{80}$, and $AUC_{30}$ were not associated with other platelet function tests, but only $T_{10\text{-}80}$ was likely associated with C/ADP, suggesting the involvement of ADP as a key agonist for thrombus formation under physiologic conditions. These findings suggest that the parameters measured in the AR chip reflect unique characteristics of individual PTF, different from those in other platelet function tests, including the PL chip. Further studies are necessary, however, to characterize the parameters in the AR chip under different conditions such as higher shear rates.

Which blood constituents might contribute to the measurements in T-TAS? With regard to CBC, high platelet counts were strongly associated with a shortened PTF time, especially in the AR chip (Table 2, Fig. 6). A previous report suggested platelet counts and aggregation responsiveness induced by ADP were related to increased coronary heart disease mortality in healthy middle-aged men [35], although other large-scale prospective studies did not detect an association [36,37]. We speculated that higher platelet counts might provide a larger platform with phospholipids for thrombin generation enhanced by agonists such as ADP released from activated platelets, resulting in the efficient and stable fibrin-rich PTF, although the clinical significance remains to be elucidated. In the PL chip, higher platelet counts are likely correlated with a lower PTF time at lower shear rates (Table 2), suggesting that platelet counts contribute to platelet aggregation in the capillary channels even in the absence of thrombin generation, especially under relatively lower shear rate conditions. It is unclear, however, how platelet counts affect the process of PTF *in vivo* under various shear rate conditions. Studies on patients with thrombocytopenia or thrombocytosis might be useful to identify the contribution of platelet counts on the T-TAS measurements. We investigated the correlation between VWF, fibrinogen, ADAMTS13, PAI-1, hs-CRP, and glycocalicin with the T-TAS measurements, but detected no significant association, except fibrinogen level, as described before. As previously reported [38], the PFA-100 results correlated with VWF activity. The VerifyNow P2Y12 assay values correlated with red blood cells, hemoglobin, and hematocrit [39] in the present study. Further studies are needed to define the blood constituents related to the parameters in the T-TAS.

The T-TAS is reportedly useful for assessment of the effects of some clinical anticoagulants, human blood products, and factor VIII

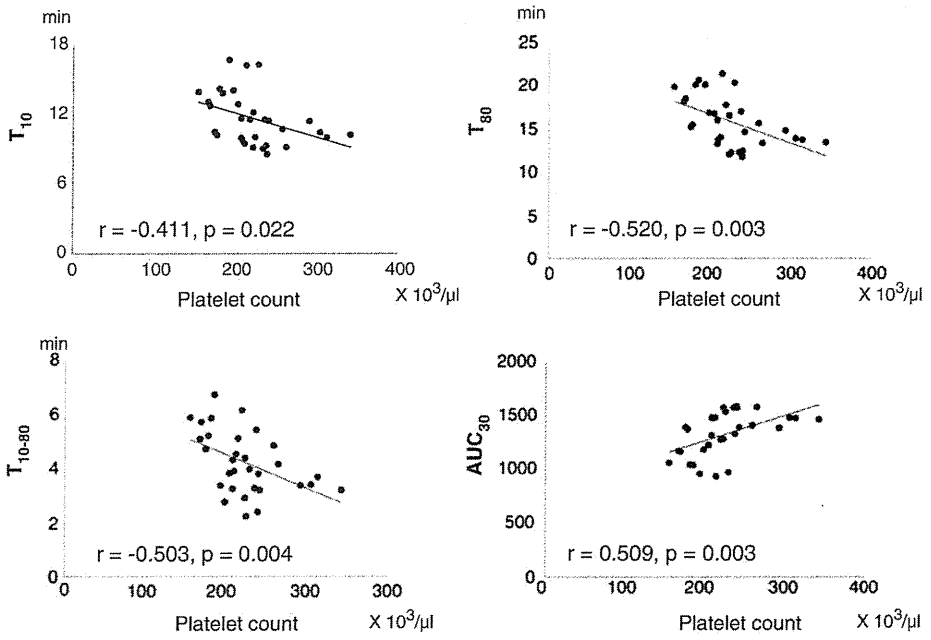


**Fig. 6.** Correlation of platelet counts and the T-TAS/AR-chip measurements, $T_{10}$ (top left), $T_{80}$ (top right), $T_{10\text{-}80}$ (bottom left), and $AUC_{30}$ (bottom right). r, correlation coefficient. p, probability value.

or IXa deficiency [18–21]. Based on the findings of the present study, the parameters measured in the T-TAS could sensitively detect individual thrombogenicity. Therefore, this system might be a promising method of evaluating not only the bleeding tendency, but also the prothrombotic status in individuals having risk factors related to atherosclerotic thrombosis, such as metabolic syndrome, diabetes, hypertension, dyslipidemia, obesity, smoking and aging. Additional clinical studies are required for further characterization.

In conclusion, we identified that the measurements obtained using the T-TAS detected the characteristics of thrombus formation under shear rate conditions in healthy individuals. These parameters might be associated with the prothrombotic status of patients with atherosclerotic diseases, and thus T-TAS might be a useful monitoring device for primary or secondary prevention of thrombotic disease.

## Conflict of Interest Statement

M. Murata: Hematology Consultant for Abbott, Advisory Committees of Daiichi-Sankyo, Advisory Committees of Sanofi-Aventis and Advisory Committees of Pfizer. T. Ohnishi and K. Hosokawa: Employees of the Fujimori Kogyo Co.

## Acknowledgements

This study was supported in part by a grant from Keio Gijuku Academic Development Funds (T.M.) and a grant from the Ministry of Health, Labor, and Welfare of Japan (M.M), and a grant from Ministry of Education, Culture, Sports, Science and Technology of Japan (M.M).

## Appendix A. Supplementary data

Supplementary data to this article can be found online at http://dx.doi.org/10.1016/j.thromres.2013.05.026.

## References

[1] Mendolicchio GL, Ruggeri ZM. New perspectives on von Willebrand factor functions in hemostasis and thrombosis. Semin Hematol 2005;42:5–14.
[2] Jackson SP. The growing complexity of platelet aggregation. Blood 2007;109(12):5087–95.
[3] Nieswandt B, Pleines I, Bender M. Platelet adhesion and activation mechanisms in arterial thrombosis and ischaemic stroke. J Thromb Haemost 2011;9(Suppl. 1):92–104.
[4] Jackson SP. Arterial thrombosis–insidious, unpredictable and deadly. Nat Med 2011;17:1423–36.
[5] Borissoff JI, Heeneman S, Kilinç E, Kassák P, Van Oerle R, Winckers K, et al. Early atherosclerosis exhibits an enhanced procoagulant state. Circulation 2010;122:821–30.
[6] Grundy SM. Pre-diabetes, metabolic syndrome, and cardiovascular risk. J Am Coll Cardiol 2012;59:635–43.
[7] Grant PJ. Diabetes mellitus as a prothrombotic condition. J Intern Med 2007;262:157–72.
[8] Lip GY, Blann AD, Edmunds E, Beevers DG. Baseline abnormalities of endothelial function and thrombogenesis in relation to prognosis in essential hypertension. Blood Coagul Fibrinolysis 2002;13:35–41.
[9] Parish S, Offer A, Clarke R, Hopewell JC, Hill MR, Otvos JD, et al. Lipids and lipoproteins and risk of different vascular events in the MRC/BHF Heart Protection Study. Circulation 2012;125:2469–78.
[10] Santilli F, Vazzana N, Liani R, Guagnano MT, Davì G. Platelet activation in obesity and metabolic syndrome. Obes Rev 2012;13:27–42.
[11] Alessi MC, Juhan-Vague I. Metabolic syndrome, haemostasis and thrombosis. Thromb Haemost 2008;99:995–1000.
[12] Dentali F, Squizzato A, Ageno W. The metabolic syndrome as a risk factor for venous and arterial thrombosis. Semin Thromb Hemost 2009;35:451–7.
[13] Nakamura K, Nakagawa H, Sakurai M, Murakami Y, Irie F, Fujiyoshi A, et al. Influence of smoking combined with another risk factor on the risk of mortality from coronary heart disease and stroke: pooled analysis of 10 Japanese cohort studies. Cerebrovasc Dis 2012;33:480–91.
[14] Mari D, Coppola R, Provenzano R. Hemostasis factors and aging. Exp Gerontol 2008;43:66–73.
[15] Michelson AD. Methods for the measurement of platelet function. Am J Cardiol 2009;103(3 Suppl.):20A–6A.
[16] Favaloro EJ, Lippi G. Coagulation update: what's new in hemostasis testing? Thromb Res 2011;127(Suppl. 2):S13–6.
[17] Cattaneo M, Hayward CP, Moffat KA, Pugliano MT, Liu Y, Michelson AD. Results of a worldwide survey on the assessment of platelet function by light transmission aggregometry: a report from the platelet physiology subcommittee of the SSC of the ISTH. J Thromb Haemost 2009;7:1029.
[18] Hosokawa K, Ohnishi T, Kondo T, Fukasawa M, Koide T, Maruyama I, et al. A novel automated microchip flow-chamber system to quantitatively evaluate thrombus formation and antithrombotic agents under blood flow conditions. J Thromb Haemost 2011;9:2029–37.
[19] Hosokawa K, Ohnishi T, Fukasawa M, Kondo T, Sameshima H, Koide T, et al. A microchip flow-chamber system for quantitative assessment of the platelet thrombus formation process. Microvasc Res 2012;83:154–61.
[20] Ogawa S, Szlam F, Ohnishi T, Molinaro RJ, Hosokawa K, Tanaka KA. A comparative study of prothrombin complex concentrates and fresh-frozen plasma for warfarin reversal under static and flow conditions. Thromb Haemost 2011;106:1215–23.
[21] Ogawa S, Szlam F, Dunn AL, Bolliger D, Ohnishi T, Hosokawa K, et al. Evaluation of a novel flow chamber system to assess clot formation in factor VIII-deficient mouse and anti-factor IXa-treated human blood. Haemophilia 2012;18:926–32.
[22] Hosokawa K, Ohnishi T, Sameshima H, Miura N, Ito T, Koide T, et al. Analysing responses to aspirin and clopidogrel by measuring platelet thrombus formation under arterial flow conditions. Thromb Haemost 2013;109:102–11.
[23] Jilma B. Platelet function analyzer (PFA-100): a tool to quantify congenital or acquired platelet dysfunction. J Lab Clin Med 2001;138:152–63.
[24] Crescente M, Di Castelnuovo A, Iacoviello L, Vermylen J, Cerletti C, de Gaetano G. Response variability to aspirin as assessed by the platelet function analyzer (PFA)-100. A systematic review. Thromb Haemost 2008;99:14–26.
[25] Wolberg AS, Aleman MM, Leiderman K, Machlus KR. Procoagulant activity in hemostasis and thrombosis: Virchow's triad revisited. Anesth Analg 2012;114(2):275–85.
[26] Bennett PC, Silverman SH, Gill PS, Lip GY. Peripheral arterial disease and Virchow's triad. Thromb Haemost 2009;101:1032–40.
[27] Ikeda Y, Handa M, Kawano K, Kamata T, Murata M, Araki Y, et al. The role of von Willebrand factor and fibrinogen in platelet aggregation under varying shear stress. J Clin Invest 1991;87:1234–40.
[28] Ruggeri ZM, Orje JN, Habermann R, Federici AB, Reininger AJ. Activation-independent platelet adhesion and aggregation under elevated shear stress. Blood 2006;108:1903–10.
[29] Favaloro EJ. Clinical utility of the PFA-100. Semin Thromb Hemost 2008;34:709–33.
[30] Ernst E, Resch KL. Fibrinogen as a cardiovascular risk factor: a meta-analysis and review of the literature. Ann Intern Med 1993;118:956–63.
[31] Dotevall A, Johansson S, Wilhelmsen L. Association between fibrinogen and other risk factors for cardiovascular disease in men and women. Results from the Göteborg MONICA survey 1985. Ann Epidemiol 1994;4:369–74.
[32] Ogiwara K, Hosokawa K, Nogami K, Matsumoto T, Shima M. Evaluation of comprehensive hemostatic function of patients with von Willebrand disease (VWD) under flow using a new microchip flow chamber system. Blood 2011;118:2283a.
[33] Ogiwara K, Nogami K, Matsumoto T, Furukawa S, Minami H, Hosokawa K, et al. Total-thrombus-formation analysis system using a microchip flow chamber reflects bleeding severity of patients with Type 1 von Willebrand disease. Blood 2012;120:2237a.
[34] Slack SM, Cui Y, Turitto VT. The effects of flow on blood coagulation and thrombosis. Thromb Haemost 1993;70:129–34.
[35] Thaulow E, Erikssen J, Sandvik L, Stormorken H, Cohn PF. Blood platelet count and function are related to total and cardiovascular death in apparently healthy men. Circulation 1991;84:613–7.
[36] Meade TW, Cooper JA, Miller GJ. Platelet counts and aggregation measures in the incidence of ischaemic heart disease (IHD). Thromb Haemost 1997;78:926–9.
[37] Spencer CG, Felmeden DC, Blann AD, Lip GY. Haemorheological, platelet and endothelial indices in relation to global measures of cardiovascular risk in hypertensive patients: a substudy of the Anglo-Scandinavian Cardiac Outcomes Trial. J Intern Med 2007;261:82–90.
[38] Kunicki TJ, Williams SA, Salomon DR, Harrison P, Crisler P, Nakagawa P, et al. Genetics of platelet reactivity in normal, healthy individuals. J Thromb Haemost 2009;7:2116–22.
[39] Voisin S, Bongard V, Tidjane MA, Lhermusier T, Carrié D, Sié P. Are P2Y12 reaction unit (PRU) and % inhibition index equivalent for the expression of P2Y12 inhibition by the VerifyNow assay? Role of haematocrit and haemoglobin levels. Thromb Haemost 2011;106:227–9.

技術論文

# 新規多項目自動血球分析装置 XN-1000 の性能評価

谷田部陽子[1)]　荒井　智子[1)]　片桐　尚子[1)]　清水　長子[1)]
林　　文明[2)]　近藤　民章[2)]　三ツ橋雄之[3)]　村田　　満[3)]

[1)]慶應義塾大学病院中央臨床検査部
[2)]シスメックス株式会社学術本部
[3)]慶應義塾大学医学部臨床検査医学

## 要　旨

新規多項目自動血球分析装置 XN-1000（シスメックス社）を試用する機会を得たので，新規測定チャンネルおよび測定モードについて性能評価，日常検査使用における有用性の検討を行った．新たに搭載されたチャンネルの検討として，1）WNR チャンネルによる有核赤血球自動補正後の白血球数と目視補正白血球数との相関，ならびに XN-1000 と目視による有核赤血球カウントとの相関，2）WDF・WPC チャンネルによる単核異常細胞検出能の評価，3）PLT-F チャンネルの低値域希釈直線性と免疫学的測定法との相関について検討した．また，新規測定モードである低値白血球モードにおいても同時再現性，低値域直線性についても検討した．WNR チャンネルの補正白血球数ならびに有核赤血球数測定は目視法と良好な相関を示した（r＝0.998，r＝0.993）．WDF・WPC チャンネルによる単核異常細胞検出では，異型リンパ球症例で 1 例の偽陰性を認めたものの，その他の症例は，単核球系異常細胞のいずれかのサスペクトメッセージが表示されていた．PLT-F チャンネルについては，低値域直線性は良好であり，かつ免疫学的測定法と良好な相関性を認めた（r＝0.969）．低値白血球モードについても，その同時再現性，低値域直線性は良好であった．日常検査業務において，目的に応じてこれら新規チャンネルやモードを使い分けることで業務の効率化を図ることができると考える．

## はじめに

近年，多項目自動血球分析装置として，多彩な機能を持った機種が開発されてきており，精度の向上だけではなく多様なニーズに対応できる自動分析装置が期待されている．今回，新規多項目自動血球分析装置 XN-1000（シスメックス社）を試用する機会を得，新規に搭載された測定チャンネルおよび測定モードについて性能評価を実施し，日常検査における有用性の検討を行ったので報告する．

Shimizu Nobuko
（〒160–8582　東京都新宿区信濃町 35 番地）
アドレス：nobuko.a.simizu@adst.keio.ac.jp
キーワード：自動血球分析装置 XN1000，NRBC，単核球，PLT-F チャンネル，低値 WBC モード
受付日：2012 年 9 月 4 日
受理日：2012 年 11 月 9 日

## 装置の特徴

XN シリーズの特徴として，新規測定チャンネルおよび新規測定モードの搭載が挙げられる．白血球計測については，WNR，WDF，WPC チャンネルおよび白血球低値モード（LW モード）が新た

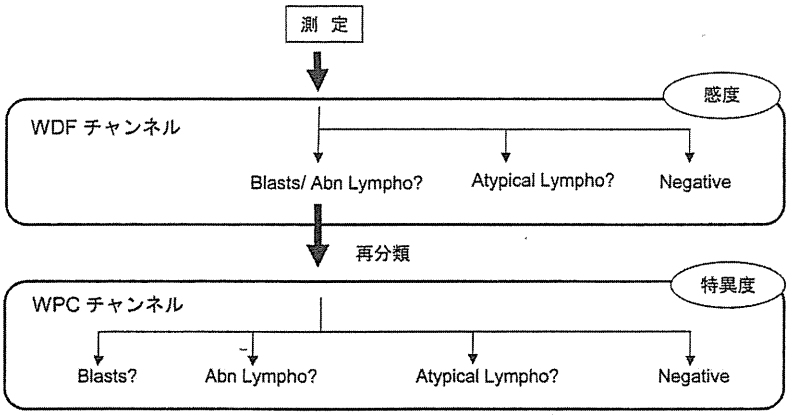


図1．WDF/WPC チャンネルによる測定フロー

に搭載されている．WNR チャンネルは，白血球（WBC），好塩基球（BASO）および有核赤血球（NRBC）を同時に計測し，NRBC 補正後の白血球数を自動的に算出する機能を持つ．WDF チャンネルは，XE シリーズの DIFF チャンネルに改良を加えたチャンネルで，リンパ球と単球の分離をより明確にし，単核球細胞の分画性能を向上させている．また，SAFLAS（形状認識フラギングアルゴリズム）解析プログラムが導入され，異常細胞を感度よく検知している．WPC チャンネルは，XE シリーズの IMI チャンネルを進化させたもので，独自のアルゴリズムにより異常細胞のフラグの特異度を向上させたチャンネルである[1]．WDF，WPC チャンネルを用いた白血球百分率測定と異常細胞の検知のフローを図1に示す．測定に際しては，まず WDF チャンネルで白血球百分率計測とともに異常単核球の有無の鑑別が行われる．異常単核球が検知され「Blast？/Abn Lympho？」にふるい分けされると，さらに WPC チャンネルにて精査が行われ，「Blast？」，「Abn Lympho？」，「Atypical Lympho？」および「Negative」に再分類される．以上の連携により，異常単核細胞のサスペクトフラグ出現精度の向上を図っている．LW モードは，全血モードに比べ計測時間を延長し白血球計測を行い，より多くの白血球を取り込むことで低値域の白血球数に対する信頼性を高めている．血小板計測に関しては，従来の PLT-I（Impedance），PLT-O（Optical）に加え，蛍光色素（オキサジン系色素）で血小板を染色しフローサイトメトリー法（FCM 法）を用いて測定する PLT-F（Fluorescence）チャンネルが搭載された．この測定法を利用することにより，従来から問題であった低値域の血小板数の測定精度の向上が図られている．

## 対象および使用機器

対象は，当院入院外来患者の残余検体および同意の得られた職員より採血した EDTA2K 加静脈血を用いた．なお，本検討は慶應義塾大学病院内の倫理委員会により承認を受けている．

検討機は，多項目自動血球分液装置 XN-1000（シスメックス社，以下 XN），対照機は，当院の現行使用機である XE-5000（シスメックス社，以下 XE）を用いた．血小板計数の検討では Cell-Dyn Sapphire（アボット社）を用いて抗 CD61 抗体による免疫学的方法にて測定を行い，対照とした．標本作製には，塗抹標本作製装置 SP-1000i（シスメックス社）を用いた．

## 方　法

### 1．WNR チャンネルにおける WBC と NRBC の検討

標本上 NRBC が WBC100 個中5個以上出現した検体（n＝64）を用いた．

1）XE で測定し目視 200 カウント中の NRBC を用いて補正した WBC と XN で測定した WBC との相関性を検討した．

2）XE で測定した WBC から算出した NRBC の絶対数（/μl）と XN で測定した NRBC の絶対数（/μl）の相関性を検討した．

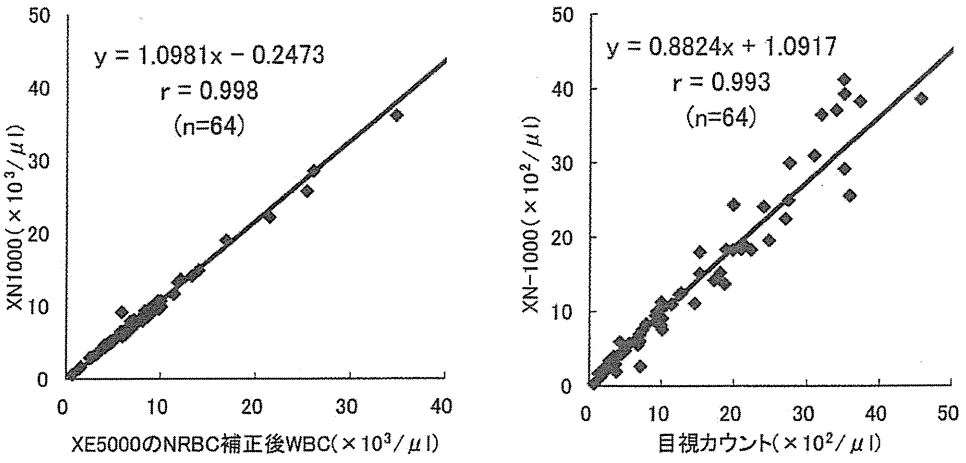


図 2. WNR チャンネルによる NRBC 出現検体の相関性

表 1. 異常リンパ球の検出（29 例）

| WDF チャンネルの判定 | Positive | | | Negative |
|---|---|---|---|---|
| WPC チャンネルの判定 | Blasts? | Abn Lympho? | Atypical Lympho? | |
| CLL（n＝11） | 2* | 10* | 0 | 0 |
| 悪性リンパ腫（n＝6） | 3 | 2 | 1 | 0 |
| 異型リンパ球出現（n＝12） | 1 | 3* | 8* | 1 |

*1 検体中に 2 種のメッセージ表示あり

2. WDF チャンネル，WPC チャンネルによる異常リンパ球の検出性能の検討

末梢血に異常細胞が出現した B 細胞リンパ腫 1 例，T 細胞リンパ腫 5 例，CLL 11 例，異型リンパ球出現症例 12 例を測定し，標本上の細胞形態と本装置におけるサスペクトメッセージの比較およびスキャッタグラムのパターンについて検討した．異型リンパ球出現症例は，目視にて異型リンパ球が 3% 以上認められた検体を用いた．

3. 血小板低値域における PLT-F チャンネルの検討

1）希釈直線性：血小板数を $50\times10^3/\mu l$ に調製した検体を 10 段階希釈し，それぞれ 2 回ずつ測定した．

2）免疫学的測定法と本装置との比較：Cell-Dyn Sapphire を用い，専用試薬である FITC 標識抗 CD61（膜糖蛋白 GPIIIa）モノクローナルマウス抗体（抗 CD61 抗体）を用いた免疫学的測定法と，本装置の PLT-I，PLT-O および新規搭載である PLT-F との相関を検討した．

4. LW モードを用いた白血球低値域の検討

1）同時再現性：白血球低値検体 2 種（600 および 1,000/μl）を LW モードにて 10 回連続測定し，変動係数を算出した．

2）希釈直線性：白血球を $1.0\times10^3/\mu l$ に調整した管理血球を 10 段階希釈し，各 10 回連続測定した．

## 結　果

1. WNR チャンネルによる WBC と NRBC の検討

1）NRBC 補正後の WBC の XE と XN の相関性は，$y=1.0981x-0.2473$，相関係数 $r=0.998$ と良好であった（図 2a）．

2）NRBC 絶対数の相関は，$y=0.8824x+1.0917$，相関係数は $r=0.993$ で，ほぼ良好であった（図 2b）．

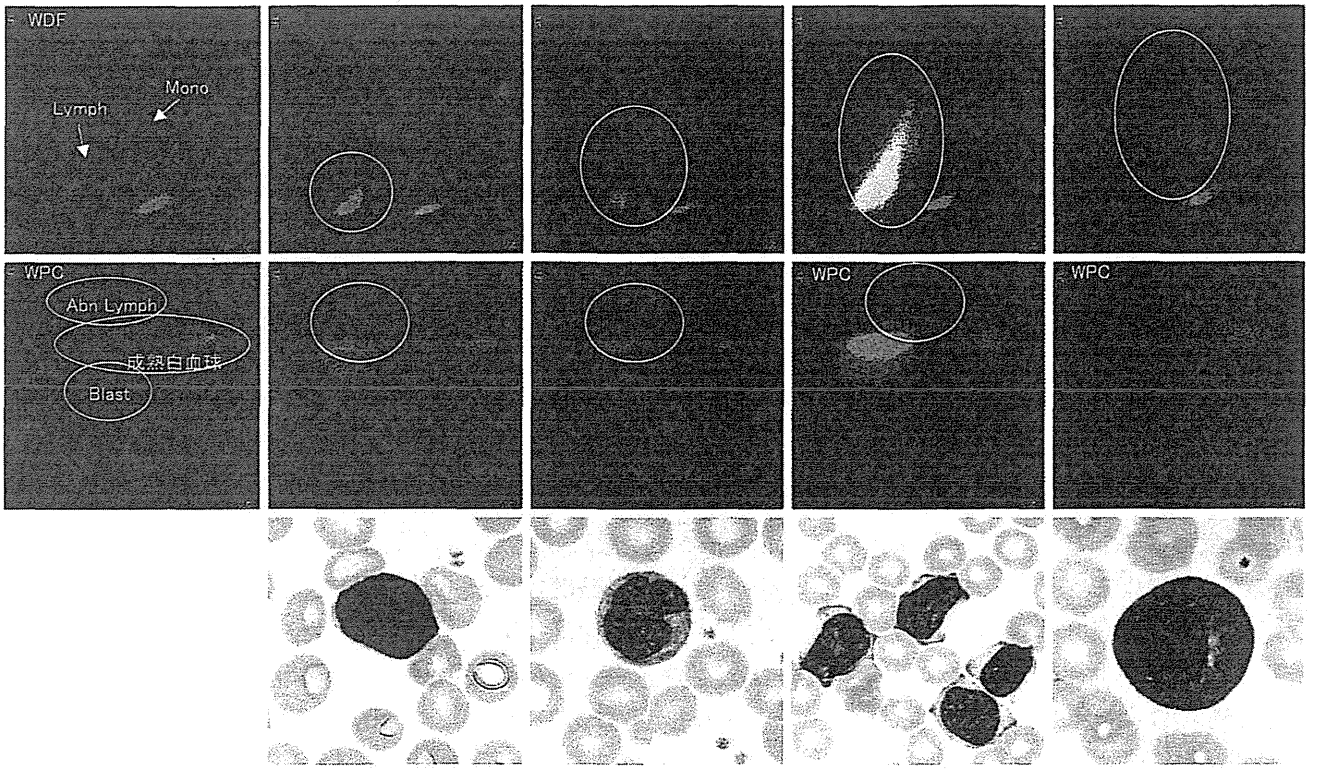


図3.　スキャッタグラムと細胞形態の典型例（上段：WDFチャンネル　下段：WPCチャンネル）

a.（WDFチャンネル）リンパ球領域のプロットが釣鐘状であった.〈異常リンパ球7%〉
b.（WDFチャンネル）リンパ球と単球のプロットがつながり，境が不明瞭である.〈異常リンパ球8%〉
c.（WDFチャンネル）多数のCLL細胞が灰色プロットとなって現れた.
（WPCチャンネル）AbnLymph領域に赤いプロットを示した.〈異常リンパ球95%〉
d.（WDFチャンネル）リンパ球から単球エリアに向かって緑とピンクが混在して伸びるプロットを示した.
（WPCチャンネル）赤いプロットの表示はない.〈異型リンパ球8%〉

## 2. WDFチャンネル，WPCチャンネルによる異常リンパ球の検出性能の検討

表1に示したように，悪性リンパ腫のサスペクトメッセージは，「Blast？」3例，「Abn Lympho？」2例，「Atypical Lympho？」1例と表示され，特異性は認められなかった．CLL症例では，11例中10例で「Abn Lympho？」と表示され，他の疾患と比較して最も適切なメッセージを示した．異型リンパ球出現症例は「Atypical Lympho？」が8例と多かったが，「Abn Lympho？」も合わせて表示した例や「Blast？」のメッセージを表示した例もあり，様々であった．また，Negativeと判定された症例の中に，目視上は異型リンパが3%存在していた例があった．スキャッタグラムは，悪性リンパ腫は症例により異なる分布を示した．典型例では，小型で核に切れ込みのある細胞がみられた症例

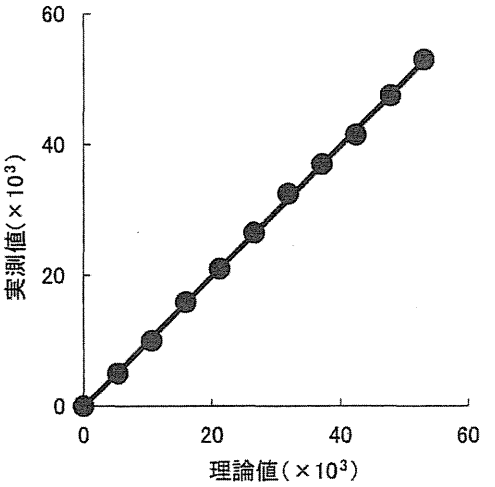


図4.　PLT-Fチャンネルによる血小板低値域の希釈直線性

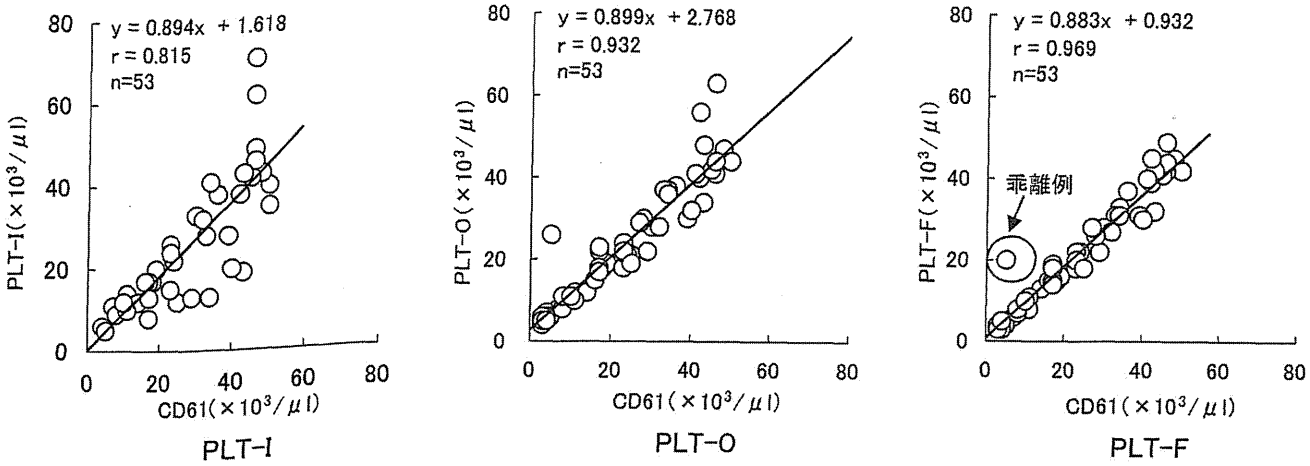


図 5. 血小板低値域における抗 CD61 抗体との相関

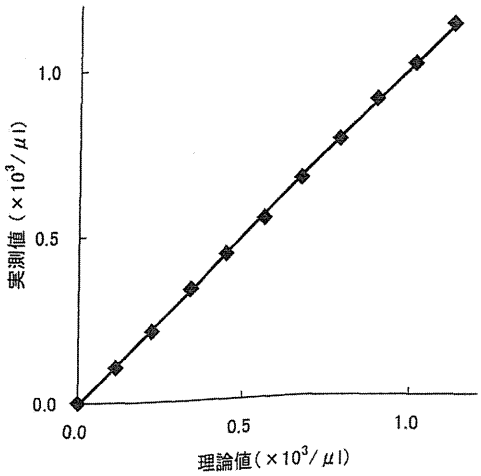


図 6. 低値域 WBC の希釈直線性

(図 3a)では，リンパ球領域のプロットが釣鐘状を示し，核膜不整の細胞がみられた症例（図 3b）では，リンパ球と単球の分離が不明確であった．図 3c の CLL はリンパ球領域から右上に伸張する灰色プロット（分類不能）を示す症例が多く認められた．また異型リンパ球出現症例では，リンパ球領域からピンク色（リンパ球）と緑色（単球）が混在して上方へ伸びてプロットされていた．

3. PLT-F チャンネルを用いた血小板低値域の検討

1) 希釈直線性は，$50\times10^3/\mu l$ 以下の低値域にて良好な直線性を示した（図 4）．

2) 抗 CD61 抗体との相関は，PLT-I の相関係数 r=0.815，PLT-O r=0.932，PLT-F r=0.969 と，PLT-F では 1 例乖離例が認められたが PLT-F の相関性が最も高い結果であった（図 5）．

4. LW モードを用いた白血球低値域の検討

1) 同時再現性は，2 検体ともに CV2.9% と良好であった．

2) 希釈直線性は，$0.1\times10^3/\mu l$ まで認められ，理論値とほぼ同じ測定値であった（図 6）．

## 考　察

新規多項目自動血球分析装置 XN-1000 に新規搭載された測定チャンネルおよび測定モードについて性能評価を行った．

WNR チャンネルは，WBC，BASO および NRBC の計測を同時に行い，NRBC 出現時に自動で白血球数を補正する機能が備わっている．XE では NRBC モードの選択が必要で，選択しない場合，WBC 数は NRBC を計り込むために NRBC 高値検体では目視カウントによる補正が必要であった．また，一般的に自動血球分析装置では NRBC と小リンパ球との判別が困難で[2]，NRBC モードにて NRBC を計測した場合でも精度に問題があった．XN の WNR チャンネルでは，専用染色液で核酸染色が行われるが，NRBC の蛍光強度は白血球より弱いために識別が可能となり，NRBC 出現例では全ての検体で白血球数の補正を行うことになった[1]．今回の検討において，補正後の WBC との相関性および XE の WBC から算出した NRBC の絶対数 (/μl) の相関はほぼ良好であった．有核赤血球出現時に WBC 補正を行う時間が短縮でき，日常検査の効率化が図れると思わ

れた．しかし，検討中には新生児でみられることのある，多数のNRBCと小リンパ球が混在する症例に遭遇しなかったため，さらなる検証が必要である．

WDFチャンネルは単核球系異常細胞を検出する感度の向上が図られ，WPCチャンネルはそれらの異常細胞とその種類を特異的に検知することを特徴とし，これらが連携することで適切なサスペクトメッセージが効率よく示されていた．自動血球分析装置による測定では小型の単核異常細胞のflag検知不良が指摘されており[3]，XEのDIFFチャンネルでもNegativeと判定されることが多く見逃されがちであった．今回，本装置では29例中28例がMorphologyでPositiveと判定した．特に，B-Cell Lymphoma（図3a）とT-Cell Lymphoma（図3b）はXEでNegativeと判定された症例であったが，XNにてPositiveに判定されており，従来機よりも細胞検知の精度の向上がみられた．これらを含めた悪性リンパ腫6症例のサスペクトメッセージは，様々であった．リンパ腫細胞の特徴は疾患により異なっており[4][5]，その多様性が現れた結果であると考えられた．CLLのサスペクトメッセージは，1例を除いて「Abn Lympho？」と，妥当であった．また，スキャッタグラムではWBC数高値の症例でリンパ球/単球分画が接合し分画不能となったため灰色プロットを示した症例が多く見受けられた（図3c）．異型リンパ球出現症例のサスペクトメッセージは，悪性リンパ腫と同様に様々であり，同一症例中でも多彩な細胞形態を示すためと考えられた．スキャッタグラムではリンパ球，単球エリアからピンク色（リンパ球）と緑色（単球）が混在し上方へ伸びるパターンが多く認められた．一方，目視で3%の異型リンパ球が認められたにもかかわらず「Negative」になった症例も存在した．詳細を検索したところ，WDFチャンネルにて「Blast？/Abn Lympho？」と判定されたがWPCチャンネルの精査で異常細胞を認めず，最終的に「Negative」と判定された症例であった．原因は，異型リンパ球の絶対数が少数（約130/μl）であったためと考えられた．

我々は，本装置の血小板計数測定PLT-Fチャンネルの測定精度についてすでに報告しているが[6]，さらに症例数を増やし検討を行った．臨床的には，血小板数の低値が問題となり[7]，また，造血器腫瘍では血小板数を1～2万/μl以上に維持するように，計画的に血小板輸血を行うのが一般的である[8]．よって，血小板数低値域の精度の高さが求められるが，低値域の直線性および低値域を中心に血小板計数の正確性が高いとされる抗CD61抗体を用いた免疫学的方法[9]と比較した相関は良好であり，従来よりも信頼性のある血小板数の報告が可能となった．1件認められた乖離例の標本上には，大小不同の血小板のほかに無構造な細胞が散見された．本例の抗CD61抗体による測定結果はメーカーより保証されており，この無構造の細胞が図りこまれたのではないかと考えられた．なお，抗CD61抗体を用いた試薬は高価であり，PLT-Fチャンネルを使用することで経済的なメリットも得られると期待される．

LWモードを用いた白血球数の同時再現性，直線性は良好な結果であった．LWモードで再検することにより，WBC低値域でも信頼性の高い結果報告が可能である．

今回検討を行った新規測定チャンネルおよび新規測定モードは，精度の高い結果が得られた．これら全てを全ルーチン検体に対して一括して実施するのは，測定時間が掛かり処理能力の低下となるが，再検などの用途に合わせて選択し利用することで，効率化が図れると考えられた．

## 結　語

XN-1000における新規測定チャンネルおよび新規測定モードの評価結果は良好であり，また次世代多項目自動血球分析装置として精度や機能性も充実し，日常検査業務においての有用性が高いと考えられた．今後，検査室の幅広い用途に対応できる機器として期待される．

## 文　献

1）越智康浩，他：多項目自動血球分析装置XN-Seriesの概要．Sysmex J　34：31—46，2011.
2）巽　典之編：計測技術ティーチング—自動血球分析装置の基本原理—　p22，克誠堂出版，東京，2006.

3) 日本検査血液学会編：スタンダード検査血液学 第2版. p139, 医歯薬出版, 東京, 2008.
4) 須知泰山, 他編：新・悪性リンパ腫アトラス p49, p75, p136, 文光堂, 東京, 2000.
5) 三輪史郎, 他：血液細胞アトラス第5版 p285—290, 文光堂, 東京, 2004.
6) 片桐尚子, 他：多項目自動血球分析装置 XN-Series における新規血小板測定チャンネルを用いた低値域血小板測定性能の検討. Sysmex J 34：62—71, 2011.
7) 清水長子, 他：これだけは知っておきたい検査のポイント第7集 Medicina 増刊号 p82—85, 医学書院, 2005.
8) 日本赤十字社 血液事業本部 医薬情報課編：輸血療法の実施に関する指針および血液製剤の使用指針 p80—91, 日本赤十字社, 2009.
9) 長田恵美里, 他：血小板数測定正確度向上のための免疫学的血小板測定の検討. 臨床病理 50 (9)：887—892, 2002.

## Abstract

### Evaluation of the performance of the new automated hematology analyzer XN-1000

Yoko Yatabe[1)], Tomoko Arai[1)], Hisako Katagiri[1)], Nobuko Shimizu[1)], Fumiaki Hayashi[2)], Tamiaki Kondo[2)], Takayuki Mitsuhashi[3)], Mitsuru Murata[3)]

[1)]Central Clinical Laboratory, Keio University Hospital, 35 Shinanomachi, Shinjuku-ku, Tokyo, Japan

[2)]Scientific Affairs, Sysmex Corporation, 1-3-2 Murotani, Nishi-ku, Kobe, Japan

[3)]Department of Laboratory Medicine, School of Medicine, Keio University, 35 Shinanomachi, Shinjuku-ku, Tokyo, Japan

We evaluated the basic performance and the clinical value of the new automated hematology analyzer XN-1000 (Sysmex), which has novel measurement channels and modes. For the new measurement channels, we examined 1) the correlations for NRBC and NRBC-corrected WBC counts between XN-1000 and the manual method (WNR channel), 2) the detectability of mononuclear abnormal cells (WDF and WPC channels) and 3) the linearity of dilution in the low value range and the correlations with the immunological PLT count method (PLT-F channel). For the new measurement mode, we evaluated the with-in run reproducibility, and the linearity of dilution in the low value range in the Low WBC mode. The correlations for NRBC and NRBC-corrected WBC counts between XN-1000 and the manual counts showed good results ($r = 0.993$ and $r = 0.998$). Regarding the detection of abnormal cells, WDF and WPC channels showed messages indicating the presence of abnormal mononuclear cells in almost all abnormal specimens, although there was one false negative case involving atypical lymphocytes. With the PLT-F channel, the linearity was fine and the new method correlated highly with the immunological method ($r = 0.969$). We also confirmed that the Low WBC mode had good with-in run reproducibility, and good linearity of dilution in the low value range. Our results suggest that the use of these different measurement methods for each sample contributes to improve the operational efficiency of routine laboratory work.

**Key words:** Automated hematology analyzer XN-1000, NRBC, Mononuclear cells, PLT-F channel, Low WBC mode

Int J Hematol (2013) 98:24–33
DOI 10.1007/s12185-013-1370-4



# Pathophysiology and management of primary immune thrombocytopenia

**Hirokazu Kashiwagi · Yoshiaki Tomiyama**

Received: 29 March 2013 / Revised: 7 May 2013 / Accepted: 13 May 2013 / Published online: 24 May 2013


**Abstract** Primary immune thrombocytopenia, or idiopathic thrombocytopenic purpura (ITP), is an autoimmune disorder characterized by isolated thrombocytopenia due to accelerated platelet destruction and impaired platelet production. Autoantibodies against platelet surface glycoproteins, such as GPIIb/IIIa and GPIb/IX complexes, play major roles in both platelet destruction and impaired platelet production, although autoantibody-independent mechanisms, such as T cell-mediated cytotoxicity, may also be involved in its pathogenesis. Recent advances in the localization of autoantigenic epitopes and the characterization of T cell functional abnormalities in ITP patients have improved our understanding of the pathophysiology of this disease. Although corticosteroids and splenectomy remain central to the treatment of ITP, a new class of drugs, i.e., thrombopoietin receptor agonists (TPO-RAs) and rituximab, have substantially broadened the therapeutic options for refractory ITP patients. Moreover, the success of TPO-RAs in ITP patients shows that reduced platelet production caused by impaired megakaryocytopoiesis plays a greater role in ITP than previously recognized.

**Keywords** Immune thrombocytopenia · Autoantibody · Epitope · Thrombopoietin receptor agonist · Rituximab

H. Kashiwagi (✉) · Y. Tomiyama
Department of Hematology and Oncology, Osaka University Graduate School of Medicine, 2-2 Yamadaoka, Suita, Osaka 565-0871, Japan
e-mail: kashi@hp-blood.med.osaka-u.ac.jp

Y. Tomiyama
Department of Blood Transfusion, Osaka University Hospital, Suita, Japan

## Introduction

Primary immune thrombocytopenia (also known as idiopathic thrombocytopenic purpura; ITP) is an autoimmune disorder characterized by isolated thrombocytopenia without abnormalities in the erythroid and myeloid/lymphoid lineages [1–3]. The incidence of ITP in adults is estimated at approximately 1.6–3.9 per 100,000 person-years [4–7]. It is conventionally thought that thrombocytopenia in ITP is caused by increased destruction of platelets opsonized by anti-platelet autoantibodies [8]. Abnormalities in megakaryocytopoiesis and impaired platelet production have also been suggested as etiologic factors [9, 10]. The remarkable success of thrombopoietin receptor agonists (TPO-RAs) for ITP patients has demonstrated that impaired platelet production plays a substantial role in ITP. Selective B cell depletion with rituximab has also been shown to be effective in the treatment of ITP. In this review, we summarize recent advances in understanding of the pathophysiology of ITP, including its autoantigenic epitopes, and the current management of primary ITP.

## Pathophysiology of primary ITP

Total platelet mass in the body is regulated by the balance between production and clearance of platelets. In hypoplastic thrombocytopenias, such as aplastic anemia or chemotherapy-induced thrombocytopenia, platelet counts are decreased due to reduced platelet production. In ITP, platelet mass shrinks as a result of accelerated platelet clearance, which is mainly due to autoantibody-mediated destruction by macrophages in spleen, and moderately impaired platelet production due to antibody- and/or

cytotoxic T cell-mediated megakaryocytic damage (Fig. 1).

## Abnormalities in B cells: production of anti-platelet autoantibodies

Historical experiments performed by Harrington and Hollingsworth in 1950 and subsequent studies, which demonstrated that the passive transfer of plasma [including immunoglobulin (Ig) G-rich fractions] from ITP patients induced the development of transient thrombocytopenia in healthy recipients, confirmed the immunologic etiology of this disease [2, 8, 11, 12]. Subsequent studies in 1970s and 80s revealed the plasma factors in question to be IgG antibodies against platelet surface glycoproteins, mainly GPIIb/IIIa and/or GPIb/IX [2]. Although plasma autoantibodies are clinically relevant, anti-platelet autoantibodies are more frequently detected in the platelet-associated (PA) form than in plasma form. The levels of PA autoantibodies, but not those of plasma autoantibodies, are correlated with the clinical course of ITP, and we and others have further shown that sera in ITP may contain antibodies against the cytoplasmic domain of GPIIIa and/or cytoplasmic proteins, such as vinculin, likely as a secondary effect of platelet destruction. Thus, in many cases, pathophysiologically important autoantibodies appear to be already bound to platelets [2, 13]. PA anti-GPIIb/IIIa and anti-GPIb/IX antibodies are detected in 43–57 % and 18–50 % in chronic ITP (cITP) patients, respectively [13, 14].

For more than two decades, efforts have been focused on identifying target epitopes for PA autoantibodies. We and others reported that PA anti-GPIIb/IIIa antibodies frequently bind to cation-dependent conformational antigens, but not to another β3 integrin, αvβ3 [2, 13]. We also demonstrated that in one-third ITP patients (11 out of 34 patients) positive for PA anti-GPIIb/IIIa antibodies, reactivity of PA anti-GPIIb/IIIa antibodies is markedly impaired with KO-variant GPIIb/IIIa (a loss-of-function mutation in the β-propeller domain of GPIIb) as compared with wild-type GPIIb/IIIa [15]. These data suggest that the β-propeller domain of GPIIb is a hot spot for autoantigenic determinants. To further clarify the epitopes, we recently performed subsequent systematic analysis of the epitopes of PA anti-GPIIb/IIIa antibodies using human–mouse chimera GPIIb/IIIa constructs, as we found that most PA anti-GPIIb/IIIa antibodies barely bind to mouse GPIIb/IIIa [16]. We detected PA anti-GPIIb/IIIa antibodies in 26 (34 %) of 76 ITP platelet eluates (PA autoantibodies eluted from washed ITP platelets by diethyl ether). We confirmed that autoantigenic epitopes are mainly localized on GPIIb, and further analyzed localization of autoantigens for 15 ITP eluates by employing various human-mouse chimera GPIIb complexed with human GPIIIa. The autoantigenic epitopes localized mainly on the N-terminal half of the β-propeller

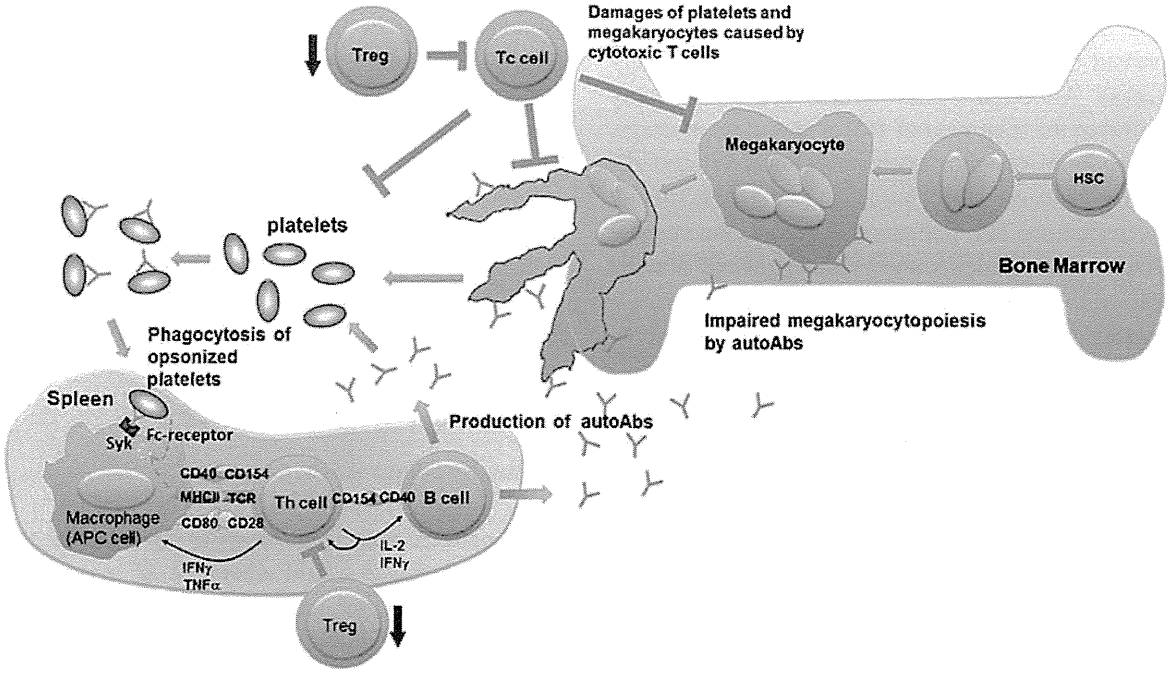


**Fig. 1** Schematic representation of pathophysiology of cITP. Opsonized platelets by autoantibodies are destroyed by macrophages in spleen and peptide fragments expressed with MHC class II stimulate helper T cells, following activation of autoreactive B cells. Impaired Tregs fail to suppress this vicious cycle. Autoantibodies also suppress megakaryocytopoiesis. Autoreactive cytotoxic T cells may play a role in the destruction of platelets and megakaryocytes. Thrombopoietin receptor (TPO-R) agonists stimulate megakaryocyte proliferation and maturation. Rituximab targets CD20-positive B cells

domain of GPIIb in all 15 patients examined (from the N-terminus to W4:4-1 loop of the β-propeller domain; L1-W235 of GPIIb) (Fig. 2). We further identified three main autoantigenic recognition sites within the region (a–c regions in Fig. 3). Interestingly, at least in three ITP patients the reactivity of autoantibodies was completely destroyed by only one amino acid substitution (R139G for two patients, and G44 N for one patient), suggesting that the target epitopes were localized on very restricted region on GPIIb in these three patients [16]. Regarding the epitopes of anti-GPIb/IX autoantibodies, He et al. [17] examined their localization by employing short linear fragments of GPIbα. They showed that six of 16 anti-GPIb/IX antibodies in ITP patients recognize a short amino acid sequence (amino acids 333–341) in GPIbα. Again, the autoantigenic epitopes for anti-GPIb-IX antibodies seem to be localized on the limited region.

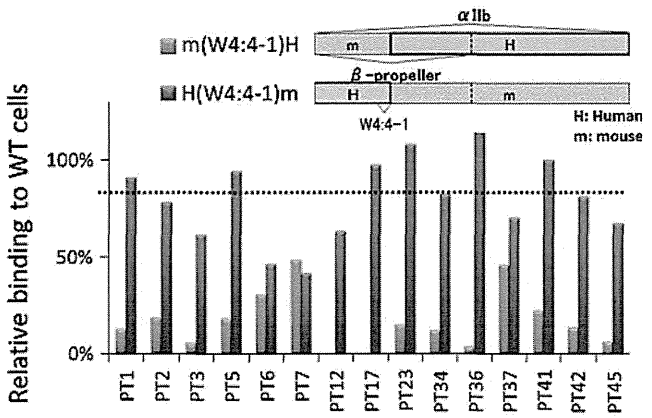


**Fig. 2** Binding of platelet-associated (PA) anti-GPIIb/IIIa antibodies in ITP patients to human-mouse chimera GPIIb/IIIa. Relative bindings of PA antibodies to 293T cells that expressed human GPIIb replaced the N-terminal half of the β-propeller domain with mouse [m(W4:4-1)H, *blue*] and 293T cells expressing mouse GPIIb replaced the N-terminal half of the β-propeller domain with human [H(W4:4-1)m, *red*] are shown

A genetic analysis of the Fab region of immunoglobulin (Ig) using phage display libraries constructed from splenocytes from cITP patients demonstrated that anti-platelet autoantibodies in cITP use highly restricted Ig variable regions [18]. We and others have also demonstrated that many of PA anti-GPIIb/IIIa antibodies show restricted $\kappa/\lambda$-chain usage [16, 19]. These data suggest that the antigenic repertoire in ITP is fairly limited and that anti-platelet antibodies are produced in limited B cell clones in many ITP patients. In HIV-, HCV- and *Helicobacter pylori* (*H. pylori*)-associated secondary ITP, cross reactivity of platelet antibodies with these pathogens has been reported [20–22]. By analogy to these secondary ITP, molecular mimicry of unknown pathogens with limited regions of platelet glycoproteins may trigger expansion of auto-reactive B cell clones in primary ITP, and autoantibody production from the B cell clones may be affected by T cell abnormalities, as described in the next section (Fig. 1).

## Abnormalities in T cells

Recently, several lines of evidences have linked T cell abnormalities to the pathogenesis of ITP. Kuwana et al. [23] demonstrated the presence of auto-reactive T cell clones against cryptic GPIIb/IIIa epitopes in cITP patients. Other studies have shown that cITP patients exhibit an imbalanced Th1/Th2 ratio [24], increase of Th17 cells and IL17 levels [25], increase of oligoclonal T cells [26], and the presence of cytotoxic T cells against autologous platelets [27].

The functions of regulatory T cells (Treg) in ITP have been extensively examined, as emergence of anti-platelet

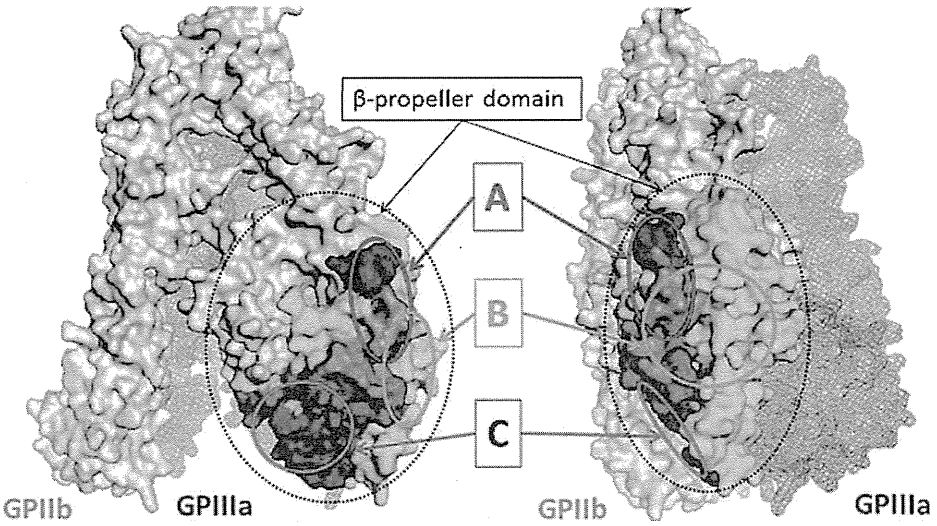


**Fig. 3** Demonstration of three major recognition sites (*A, B and C*) of PA anti-GPIIb/IIIa autoantibodies in ITP patients. Shown is a crystal structure of the resting form of GPIIb/IIIa with two different angles made by PyMOL Version 1.4 software (DeLano Scientific LLC). The N-terminal half and the whole region of the β-propeller domain of GPIIb are indicated in *yellow* and by the *dotted circle*, respectively. Each loop essential for PA antibody bindings is *distinctly colored*

autoantibodies and anti-platelet cytotoxic T cells is an expected consequence of the loss of immunological tolerance to self-antigens. Tregs are T cells marked by $CD4^+CD25^+Foxp3^+$, which account for 5–10 % of the peripheral $CD4^+$ T cell population and play essential roles in self-tolerance by suppression of cell- and antibody-mediated immune responses [28]. Several reports demonstrated reduction in Treg numbers and/or impairment of Treg function in ITP patients [29, 30]. Very recently, Nishimoto et al. [31] demonstrated that approximately 40 % of Treg-deficient mice became thrombocytopenic, which lasted for up to 5 weeks. The thrombocytopenic mice displayed IgG anti-platelet antibodies, which predominantly react to GPIb/IX, and transfer of purified Tregs into the mice prevented thrombocytopenia [31, 32]. Stasi et al. [33] demonstrated that a reduced number and a defective suppressive capacity of Tregs in ITP patients were restored in responders of rituximab, suggesting abnormalities in Tregs in ITP patients may be regulated by interaction between T and B cells.

## Mechanism of accelerated platelet clearance

Opsonized platelets by anti-platelet IgG antibodies are destructed mainly by macrophages in spleen via low-affinity Fc receptors, FcγRIIA and FcγRIIIA [34]. FcγRIIA and FcγRIIIA have immunoreceptor tyrosine-based activation motif (ITAM) in the cytoplasmic regions, and phosphorylation of ITAM domain induced by Fc binding, followed by Syk phosphorylation, activates phagocytosis [35]. Several reports have also suggested the involvement of another inhibitory FcγR, FcγRIIB, in the control of phagocytosis. FcγRIIB contains an immunoreceptor tyrosine-based inhibitory motif (ITIM) and inhibits phagocytosis and pro-inflammatory cytokine release by monocytes/macrophages and dendritic cells. Samuelsson et al. [36] showed that FcγRIIB on splenic macrophages is required for the protective effects of intravenous immunoglobulin against platelet consumption in a murine ITP model. Sifting of the monocyte FcγR balance toward the inhibitory FcγRIIB has been also demonstrated in ITP patients responded to *H. pylori* eradication [37] or high-dose dexamethasone treatment [38]. In addition to Fc-mediated phagocytosis, platelet autoantibodies may fix complements, enhancing opsonization or facilitating direct platelet lysis [39–41]. Moreover, Nardi et al. [20] showed that anti-GPIIIa antibodies found in an HIV-associated ITP patient caused platelet destruction via induction of reactive oxygen species (ROS), and that these mechanisms may also contribute to primary ITP. Some patients with ITP lack detectable anti-platelet autoantibodies, and platelet clearance in these cases may result from $CD8^+$ T cell-mediated cytotoxicity [27, 42].

## Impaired platelet production

Impairment of platelet production in ITP patients has been demonstrated directly or indirectly by morphological studies of megakaryocytes, megakaryocytic colony formation and platelet kinetic studies.

### *Abnormalities in morphology of megakaryocytes*

Morphological abnormalities in megakaryocytes of cITP patients, e.g. increase of immature megakaryocytes, disappearance of platelet production, and degenerative change of nucleus and cytoplasm, have been observed by optical microscopic analysis since the 1940s [2]. Ultrastructural analysis of megakaryocytes of 11 ITP patients showed extensive apoptotic and para-apoptotic changes, such as dilation of endoplasmic reticulum, swollen mitochondria, dilation of the demarcation membrane system, nuclear fragmentation and chromatin condensation, in about 80 % of ITP megakaryocytes [43]. These (para-)apoptotic changes can be induced in megakaryocytes obtained by suspension culture of $CD34^+$ cells with ITP plasma [43].

### *Suppression of megakaryocytopoiesis*

Since the expression levels of GPIb/IX and GPIIb/IIIa increases during the maturation process of megakaryocytes [44], it is very plausible that anti-platelet autoantibodies against GPIb/IX and/or GPIIb/IIIa attack megakaryocytes as well as platelets. Two in vitro studies using megakaryocyte culture systems from cord blood-derived $CD34^+$ cells showed that autoantibodies against anti-GPIb/IX and GPIIb/IIIa in ITP patients reduce megakaryocyte production and maturation [45, 46]. Antibodies bound to megakaryocytes may induce apoptosis via ROS production and/or activation of the PI3 K/Akt pathway, in addition to antibody-dependent cellular toxicity and complement-dependent cytotoxicity [47]. In contrast, Yang et al. [48] demonstrated that most ITP plasma boosts megakaryocyte quantity but impairs megakaryocyte maturation, resulting in significantly less polyploidy cells and platelet release, and that cell apoptosis is inhibited in these immature megakaryocytes. Megakaryocytes in ITP patients may also be attacked by cytotoxic T cells in bone marrow [49].

### *Platelet kinetic studies and serum (plasma) thrombopoietin concentration*

Intensive studies of platelet kinetics using $^{111}$indium-labeled autologous platelet transfusion were performed in 1980s, and showed that platelet production remains normal or is decreased in two-thirds of cITP patients compared with normal subjects [9, 50], suggesting that accelerated

platelet clearance may not be the sole etiologic factor underlying thrombocytopenia in ITP. We assessed platelet turnover and production using reticulated platelets, which are RNA-rich young platelets stained with thiazole orange, by flow cytometry (FCM) [51]. Percentage (RP %) and absolute number (RP number) of reticulated platelets represent turnover and production of platelets, respectively. In cITP patients, RP % was markedly increased compared with healthy control (healthy control 7.7 ± 2.7 %, cITP 23.8 ± 11.6, $P < 0.001$), whereas RP number was decreased (control 17.0 ± 6.6 × $10^3$/μl, cITP 8.3 ± 4.6, $P < 0.05$). These data confirm that both rapid platelet turnover and impaired platelet production occur in ITP patients. Two methods are available for measuring RNA-rich platelets: the RP % method using FCM and the IPF % method (immature platelet fraction) performed using the Sysmex XE-2100 (or XE-5000) autoanalyzer. We have compared these two methods in parallel for their utility in differential diagnosis between ITP and AA. The sensitivity (82 %) and specificity (93 %) of the RP % method for the diagnosis of ITP were much better than those of the IPF % method (sensitivity 67 %, specificity 63 %). Although IPF % is measured automatically and easy to use, we should take its moderate sensitivity and specificity into account [52].

TPO is the major physiologic regulator of platelet production, and it is continuously synthesized and secreted predominantly in the liver, with no translational or post-translational regulation [53, 54]. Serum (plasma) TPO level is regulated by consumption of TPO by its binding to the TPO receptor (c-Mpl) on platelets or megakaryocytes. When platelet mass increases, the relative amount of TPO to megakaryocytes decreases, leading to suppression of platelet production. Conversely, when platelet mass is reduced, the relative amount of TPO to megakaryocytes rises. These mechanisms, referred to collectively as "the sponge theory", contribute to homeostasis of platelet number. In fact, TPO levels of patients with aplastic anemia or chemotherapy-induced thrombocytopenia are markedly elevated. In contrast, TPO levels are not elevated, or only slightly elevated, in patients with ITP [51, 55]. Taken together with the moderately impaired platelet production in ITP, relatively low levels of TPO indicate that ITP may represent a good candidate for treatment with TPO-RAs.

## Current management of ITP

Differences in the rates of platelet count increase following *H. pylori* eradication in ITP have been reported for different regions. In Japan, *H. pylori* screening and eradication appear to be warranted, given the high background prevalence of *H. pylori* infection and the high platelet response rate to eradication, whereas in the United States and Europe its value is uncertain [56]. Such inter-ethnic differences should be considered when developing treatment guidelines for chronic ITP. In this context, a reference guide for management of adult cITP was published in 2012 by the study group of the Specific Disease Treatment Research Program for Intractable Diseases of the Ministry

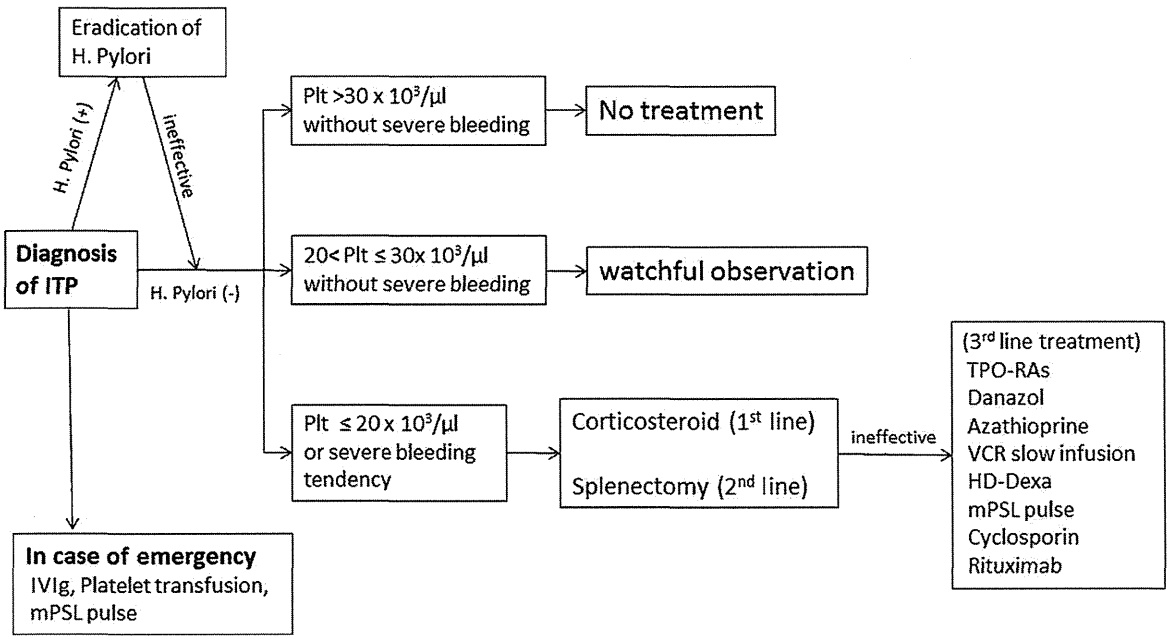


**Fig. 4** The 2012 reference guide for management of adult cITP published from the study group of the Specific Disease Treatment Research Program for Intractable Diseases of the Ministry of Health Labour and Welfare of Japan. *IVIg* intravenous immunoglobulin, *mPSL* methylprednisolone, *VCR* vincristine, *HD-Dexa* high-dose dexamethasone

of Health, Labour, and Welfare in Japan (Fig. 4). The reference guide corresponds in large part with a recently published international consensus report [3], except eradication of *H. pylori*. When *H. pylori* is negative or platelet response to the eradication is not obtained, these guidelines recommend starting treatment if platelet counts fall below 20–30 $\times$ $10^3$/μL, and/or severe bleeding is observed. First line treatment is corticosteroids, usually prednisolone, although complete remission, which is defined as more than 100 $\times$ $10^3$/μl without medication, would be achieved in only ~20 % of patients. Splenectomy is recommended for corticosteroid-resistant patients as a second-line treatment. Splenectomy has a 60-year record of success for achieving durable remissions in approximately two-thirds of patients [57]. For refractory ITP patients in whom corticosteroids and splenectomy fail, many drugs have been tried as third-line treatments, including TPO-RAs and rituximab, although only TPO-RAs are approved for the treatment of ITP in Japan.

## TPO-RAs

Recombinant human TPO (rhTPO) and pegylated recombinant human megakaryocyte growth and development factor (PEG-rHuMGDF) were developed for clinical studies in thrombocytopenic disorders [53]. PEG-rHuMGDF is a truncated form of TPO that contains the first 163 amino acids of endogenous TPO. However, PEG-rHuMGDF paradoxically induced persistent thrombocytopenia in 13 of 325 healthy volunteers. This thrombocytopenia was caused by an antibody to PEG-rHuMGDF that cross-reacted with endogenous TPO and neutralized its biological activity [58]. Although rhTPO did not show such adverse effects, the development of both rhTPO and PEG-rHuMGDF was stopped in 1998. Subsequently, efforts to produce safer TPO-related products continued, and we are now able to use two TPO-RAs for refractory ITP patients in the clinical setting [59, 60].

### *Eltrombopag*

Eltrombopag is an orally available small non-peptide molecule with a molecular weight of 546 Da. It was identified by screening of large libraries of small non-peptide molecules for the ability to stimulate STATs in TPO-dependent cell lines [61]. Eltrombopag binds to the transmembrane region of the TPO receptor, and activates JAK/STAT and RAS/RAF/MAPK pathways [59].

A double-blind, placebo-control study in adults with ITP patients with platelet counts of lower than 30,000/μL (RAISE study) showed ~80 % patients in the eltrombopag group responded to treatment at least once during the study, compared with 28 % patients in the placebo group [62]. Importantly, similar responses were obtained irrespective of splenectomy status and 59 % of patients in the eltrombopag group could reduce concomitant treatment (mostly corticosteroids). Three (2 %) out of 135 patients receiving eltrombopag had thromboembolic events [2 pulmonary embolism (PE) and 1 deep-vein thrombosis (DVT)]. Nine (7 %) and five (4 %) eltrombopag-treated patients showed mild increases in alanine aminotransferase and total bilirubin, respectively. A recently published long-term study (median 100 weeks) of eltrombopag (EXTEND study) showed maintenance of high efficiency (254/299, 85 %) of eltrombopag in long-term use [63]. Twenty-one thromboembolic events [nine deep-vein thrombosis (DVT), five central nervous system ischemic events, four myocardial infarction, and three pulmonary embolisms (PE)] were reported in sixteen (16 %) patients and two patients were diagnosed with lymphoma.

Patient ethnicity may affect the pharmacokinetics of eltrombopag. AUC exposure to eltrombopag was approximately twofold greater among Japanese healthy volunteers than among non-Asian (predominantly Caucasian) volunteers, and 87 % greater among ITP patients of East Asian descent compared to non-East Asian ITP patients [64, 65]. Multiple factors, including body weight differences and genetic differences in metabolizing enzymes such as UGT1A1, UGT1A3, CYP1A2, and CYP2C8 and transporters, may contribute to the differences between Japanese and Caucasian patients [64]. From these data, it has been recommended that for patients of East Asian ancestry (such as Japanese, Korean, Chinese, and Taiwanese) the initial dose of eltrombopag should be reduced to 25 mg once daily. Notably, a recent Japanese clinical trial evaluated the efficacy and safety of eltrombopag at a starting dose of 12.5 mg and a maximum dose of 50 mg in the treatment of Japanese patients with previously treated chronic ITP [66]. During the first 3 weeks treated with 12.5 mg eltrombopag, 22 % (5/23) of Japanese patients responded. Since the disease state is chronic in nature and only 12.5 mg tablets are available in Japan to date, it is possible that 25 mg every-other-day administration as a starting dose may be suitable for some chronic ITP patients of East Asian ancestry to prevent overshooting of platelet count.

### *Romiplostim*

Romiplostim is a rationally designed "peptibody" composed of an Fc fragment with two identical peptide sequences linked via polyglycine covalently bound at residue 228 of the heavy chain [59]. Its half-life is substantially lengthened by the Fc fragments, and it is administered subcutaneously once a week. Romiplostim competitively binds to the TPO receptor with intrinsic TPO, but the receptor-binding peptide component shows